https://ntrs.nasa.gov/search.jsp?R=19930091677 2020-06-17T02:23:58+00:00Z

NATIONAL ADVISORY COMMITTEE FOR AERONAUTICS

REPORT No. 603

WIND-TUNNEL INVESTIGATION OF WINGS WITH ORDINARY AILERONS AND FULL-SPAN EXTERNAL-AIRFOIL FLAPS

By ROBERT C. PLATT and JOSEPH A. SHORTAL

1937

For sale by the Superintendent of Documents, Washington, D. C. - - - - - - - - - - - - - - Price 10 cents
Subscription price, $3 per year

AERONAUTIC SYMBOLS

1. FUNDAMENTAL AND DERIVED UNITS

	Symbol	Metric		English	
		Unit	Abbreviation	Unit	Abbreviation
Length	l	meter	m	foot (or mile)	ft. (or mi.)
Time	t	second	s	second (or hour)	sec. (or hr.)
Force	F	weight of 1 kilogram	kg	weight of 1 pound	lb.
Power	P	horsepower (metric)		horsepower	hp.
Speed	V	kilometers per hour	k.p.h.	miles per hour	m.p.h.
		meters per second	m.p.s.	feet per second	f.p.s.

2. GENERAL SYMBOLS

W, Weight$=mg$

g, Standard acceleration of gravity$=9.80665$ m/s^2 or 32.1740 ft./sec.^{2}

m, Mass$=\frac{W}{g}$

I, Moment of inertia$=mk^2$. (Indicate axis of radius of gyration k by proper subscript.)

μ, Coefficient of viscosity

ν, Kinematic viscosity

ρ, Density (mass per unit volume)

Standard density of dry air, 0.12497 kg-m^{-4}-s^2 at 15° C. and 760 mm; or 0.002378 lb.-ft.$^{-4}$ sec.^{2}

Specific weight of "standard" air, 1.2255 kg/m^3 or 0.07651 lb./cu. ft.

3. AERODYNAMIC SYMBOLS

S, Area

S_w, Area of wing

G, Gap

b, Span

c, Chord

$\frac{b^2}{S}$, Aspect ratio

V, True air speed

q, Dynamic pressure$=\frac{1}{2}\rho V^2$

L, Lift, absolute coefficient $C_L=\frac{L}{qS}$

D, Drag, absolute coefficient $C_D=\frac{D}{qS}$

D_0, Profile drag, absolute coefficient $C_{D_0}=\frac{D_0}{qS}$

D_i, Induced drag, absolute coefficient $C_{D_i}=\frac{D_i}{qS}$

D_p, Parasite drag, absolute coefficient $C_{D_p}=\frac{D_p}{qS}$

C, Cross-wind force, absolute coefficient $C_C=\frac{C}{qS}$

R, Resultant force

i_w, Angle of setting of wings (relative to thrust line)

i_t, Angle of stabilizer setting (relative to thrust line)

Q, Resultant moment

Ω, Resultant angular velocity

$\rho\frac{Vl}{\mu}$, Reynolds Number, where l is a linear dimension (e.g., for a model airfoil 3 in. chord, 100 m.p.h. normal pressure at 15° C., the corresponding number is 234,000; or for a model of 10 cm chord, 40 m.p.s., the corresponding number is 274,000)

C_p, Center-of-pressure coefficient (ratio of distance of c.p. from leading edge to chord length)

α, Angle of attack

ϵ, Angle of downwash

α_0, Angle of attack, infinite aspect ratio

α_i, Angle of attack, induced

α_a, Angle of attack, absolute (measured from zero-lift position)

γ, Flight-path angle

REPORT No. 603

WIND-TUNNEL INVESTIGATION OF WINGS WITH ORDINARY AILERONS AND FULL-SPAN EXTERNAL-AIRFOIL FLAPS

By ROBERT C. PLATT and JOSEPH A. SHORTAL
Langley Memorial Aeronautical Laboratory

148122—37——1

NATIONAL ADVISORY COMMITTEE FOR AERONAUTICS

HEADQUARTERS, NAVY BUILDING, WASHINGTON, D. C.

LABORATORIES, LANGLEY FIELD, VA.

Created by act of Congress approved March 3, 1915, for the supervision and direction of the scientific study of the problems of flight (U. S. Code, Title 50, Sec. 151). Its membership was increased to 15 by act approved March 2, 1929. The members are appointed by the President, and serve as such without compensation.

JOSEPH S. AMES, Ph. D., *Chairman*,
Baltimore, Md.

DAVID W. TAYLOR, D. Eng., *Vice Chairman*,
Washington, D. C.

WILLIS RAY GREGG, Sc. D., *Chairman, Executive Committee*,
Chief, United States Weather Bureau.

CHARLES G. ABBOT, Sc. D.,
Secretary, Smithsonian Institution.

LYMAN J. BRIGGS, Ph. D.,
Director, National Bureau of Standards.

ARTHUR B. COOK, Rear Admiral, United States Navy,
Chief, Bureau of Aeronautics, Navy Department.

FRED D. FAGG, JR., J. D.,
Director of Air Commerce, Department of Commerce.

HARRY F. GUGGENHEIM, M. A.,
Port Washington, Long Island, N. Y.

SYDNEY M. KRAUS, Captain, United States Navy,
Bureau of Aeronautics, Navy Department.

CHARLES A. LINDBERGH, LL. D.,
New York City.

WILLIAM P. MACCRACKEN, J. D.,
Washington, D. C.

AUGUSTINE W. ROBINS, Brigadier General, United States Army,
Chief Matériel Division, Air Corps, Wright Field, Dayton, Ohio.

EDWARD P. WARNER, M. S.,
Greenwich, Conn.

OSCAR WESTOVER, Major General, United States Army,
Chief of Air Corps, War Department.

ORVILLE WRIGHT, Sc. D.,
Dayton, Ohio.

GEORGE W. LEWIS, *Director of Aeronautical Research*

JOHN F. VICTORY, *Secretary*

HENRY J. E. REID, *Engineer in Charge, Langley Memorial Aeronautical Laboratory, Langley Field, Va.*

JOHN J. IDE, *Technical Assistant in Europe, Paris, France*

TECHNICAL COMMITTEES

AERODYNAMICS
POWER PLANTS FOR AIRCRAFT
AIRCRAFT MATERIALS
AIRCRAFT STRUCTURES
AIRCRAFT ACCIDENTS
INVENTIONS AND DESIGNS

Coordination of Research Needs of Military and Civil Aviation

Preparation of Research Programs

Allocation of Problems

Prevention of Duplication

Consideration of Inventions

LANGLEY MEMORIAL AERONAUTICAL LABORATORY

LANGLEY FIELD, VA.

Unified conduct, for all agencies, of scientific research on the fundamental problems of flight.

OFFICE OF AERONAUTICAL INTELLIGENCE

WASHINGTON, D. C.

Collection, classification, compilation, and dissemination of scientific and technical information on aeronautics.

REPORT No. 603

WIND-TUNNEL INVESTIGATION OF WINGS WITH ORDINARY AILERONS AND FULL-SPAN EXTERNAL-AIRFOIL FLAPS

By Robert C. Platt and Joseph A. Shortal

SUMMARY

An investigation was carried out in the N. A. C. A. 7- by 10-foot wind tunnel of an N. A. C. A. 23012 airfoil equipped, first, with a full-span N. A. C. A. 23012 external-airfoil flap having a chord 0.20 of the main airfoil chord and with a full-span aileron with a chord 0.12 of the main airfoil chord on the trailing edge of the main airfoil and equipped, second, with a 0.30-chord full-span N. A. C. A. 23012 external-airfoil flap and a 0.13-chord full-span aileron. The results are arranged in three groups, the first two of which deal with the airfoil characteristics of the two airfoil-flap combinations and with the lateral-control characteristics of the airfoil-flap-aileron combinations. The third group of tests deals with several means for balancing ailerons mounted on a special large-chord N. A. C. A. 23012 airfoil model with and without a 0.20-chord N. A. C. A. 23012 external-airfoil flap. The tests included an ordinary aileron, a curtained-nose balance, a Frise balance, and a tab.

The results obtained for the 0.30 c_w flap verify the conclusion made from previous tests of the 0.20 c_w flap combination, namely, that external-airfoil flaps applied to the N. A. C. A. 230 airfoil sections give characteristics more favorable to speed range, to low power requirements in flight at high lift coefficients, and to low flap-operating moments than do other types of flap in general use. The ailerons can produce large rolling moments with relatively small adverse yawing moments in flight conditions ranging from high speed to minimum speed. The nose balance and Frise balance were ineffective in reducing the stick forces required for a given control effectiveness, but the use of tabs in combination with a differential aileron motion provided a means of obtaining desirable stick forces throughout the flight range. The aerodynamic advantages of this aileron-flap combination appear to outweigh probable design difficulties.

INTRODUCTION

Improvement of airplane speed range and performance by the use of trailing-edge high-lift devices has been hampered by the necessary compromise between obtaining the highest possible maximum lift coefficient and the necessity of providing at least a minimum of lateral control. The usual compromise has involved the use of flaps over the central portion of the span with ailerons attached to the tip portion. This procedure results not only in the direct loss of possible maximum lift over the unflapped area but may lead to an additional hazard resulting from the tendency of partial-span flaps of the conventional type to reduce, in some cases, the degree of stability and control near the stall. It is therefore generally recognized that the development of a lateral-control arrangement that can be used in combination with a full-span flap offers definite possibilities for improvements in speed range and safety.

In most of the numerous attempts that have been made to devise such an arrangement (for example, references 1, 2, and 3) unforeseen difficulties have practically canceled the anticipated improvement. In some cases reductions of maximum lift or increases in minimum drag have had to be accepted in order to obtain the minimum acceptable lateral control; the mechanical complications or operational difficulties of other arrangements have prevented their satisfactory application. At present no combination that makes full use of the capabilities of high-lift devices and provides satisfactory lateral control has found general application to airplane design.

The investigation reported herein dealt with an arrangement that, on preliminary study, indicated possibilities of meeting the foregoing requirements. The arrangement consisted of a main airfoil on the trailing edge of which were an external-airfoil flap and ailerons forming the lip of the slot between the main airfoil and the flap. This combination logically results from an attempt to combine the desirable characteristics of the slot-lip ailerons described in reference 3 with those of the external-airfoil flaps described in reference 4. These ailerons being structurally similar to ordinary ailerons, relatively complicated mechanical and structural arrangements are avoided and the main airfoil contour is left unbroken when the ailerons are undeflected, thus making available the full capabilities of external-airfoil flaps for speed-range improvement and reduction of power requirements in low-speed flight.

This wind-tunnel investigation was divided into three general phases:

1. Measurement of the lift, drag, and pitching-moment characteristics and the flap hinge moments of an N. A. C. A. 23012 airfoil with N. A. C. A. 23012

external-airfoil flaps having chords (c_f) that are 0.20 and 0.30 of the main airfoil chord (c_w).

2. In addition to the characteristics measured in the first phase, the measurement of the rolling- and yawing-moment characteristics of the foregoing combinations provided with ailerons having chords (c_a) of 0.12 and 0.13 of the main airfoil chord and deflected various amounts. (The aileron chord was made 10 percent of the over-all airfoil chord in each case to permit the results to be directly compared with the data of reference 3.)

3. Measurement of aileron hinge moments and lift and drag increments of a wide-chord N. A. C. A. 23012 airfoil with and without a 0.20 c_w external-airfoil flap. Various types of aileron balance were tested.

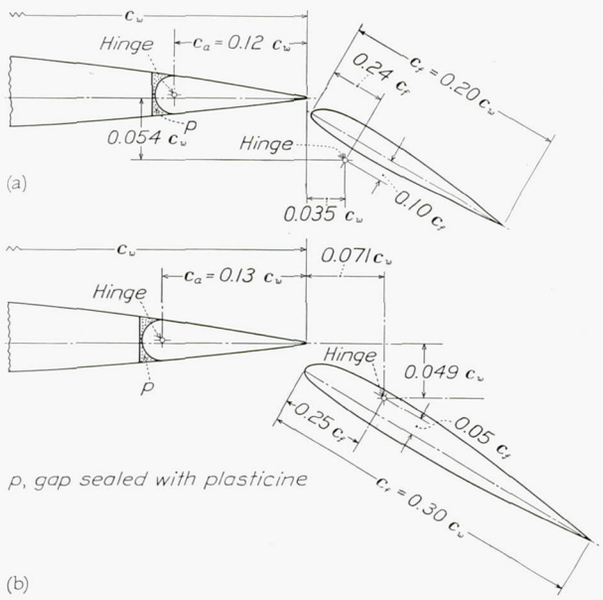

(a) N. A. C. A. 23012 airfoil with 0.20 c_w N. A. C. A. 23012 external-airfoil flap and 0.12 c_w ordinary ailerons.

(b) N. A. C. A. 23012 airfoil with 0.30 c_w N. A. C. A. 23012 external-airfoil flap and 0.13 c_w ordinary ailerons.

FIGURE 1.—Ailerons and flaps tested.

The results obtained have been studied with the purpose of clarifying the fundamental phenomena involved in the operation of the general type of device tested. They further provide the information necessary for comparison of the particular arrangement tested with other devices intended to accomplish the same purpose. Certain difficulties that may be encountered in flight applications of the device are pointed out and some investigation of methods of overcoming these difficulties is discussed.

APPARATUS AND METHODS

The investigation was carried out in the N. A. C. A. 7- by 10-foot open-throat wind tunnel (reference 5). The models used in the first phase of the investigation consisted of the following:

(1) A rectangular N. A. C. A. 23012 airfoil of 10-inch chord and 60-inch span, constructed of laminated mahogany.

(2) One 2-inch-chord and one 3-inch-chord duralumin N. A. C. A. 23012 airfoil, each having a span of 60 inches. These small airfoils served as flaps.

The tests of the combination using the 2-inch-chord flap are described in reference 4; the data have been included in this report for completeness. Exactly similar methods were adopted for the tests of the combination using the 3-inch-chord flap; surveys were made to determine the effect of flap position and angle, a desirable flap-hinge-axis location was selected from contours similar to those in reference 4, and force tests were made to determine the characteristics of the finally selected arrangement at various flap angles. In order to avoid section inaccuracies during the final force tests, these tests were completed before ailerons were built into the trailing edge of the main airfoil.

For the second phase of the investigation the trailing edge of the main airfoil was cut off and ailerons extending across the full 60-inch span of the airfoil were installed. For the tests with the 2-inch flap the chord of the ailerons (back of the hinge) was 1.2 inches; for the tests with the 3-inch flap it was 1.3 inches. The 1.2-inch-chord ailerons were made of the wooden section taken from the trailing edge of the main airfoil but difficulty in maintaining accurate settings of these ailerons indicated the desirability of using duralumin for the wider-chord ailerons. The settings of the 1.3-inch ailerons were probably somewhat more accurate than those of the 1.2-inch ailerons for this reason. Figure 1 shows pertinent details of the models used. Figure 2 is a photograph of the model with the 2-inch flap and 1.2-inch ailerons. If the details relating to the ailerons are disregarded, the figures show the condition of the models in the first phase of the investigation.

A series of tests in which angle of attack, aileron deflection, and flap angle were varied over the useful

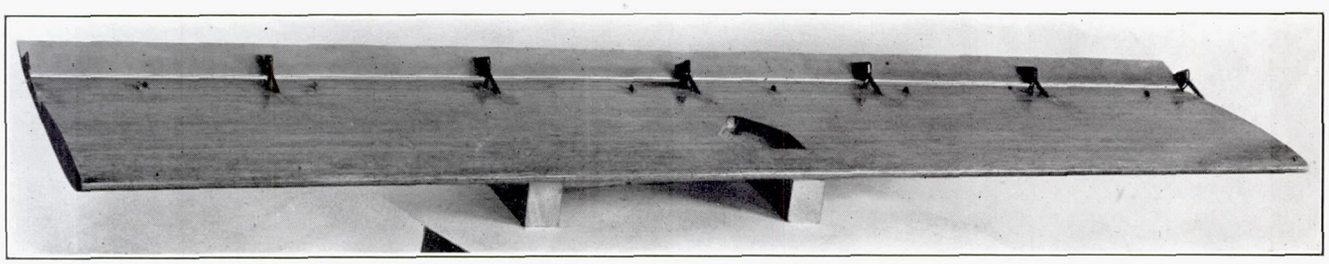

FIGURE 2.—Model N. A. C. A. 23012 airfoil with 0.20 c_w N. A. C A. 23012 external-airfoil flap and 0.12 c_w ordinary aileron.

ranges was made for each wing-flap-aileron combination. The deflection of one half-span aileron was varied from the selected maximum up to the maximum down deflection. The effect of moving both ailerons simultaneously may be obtained by the addition of the effects produced by one aileron deflected to each of the assumed settings, due account being taken of the signs of moments and deflections. This method of obtaining rolling, yawing, and hinge moments of ailerons deflected in various ways from the data for one aileron is explained in detail in reference 2.

All tests involved in the first two phases were conducted according to standard force-test procedure in the 7- by 10-foot tunnel (reference 5). The dynamic pressure in the jet was maintained at 16.37 pounds per square foot corresponding to a speed of 80 miles per hour in standard air. The test Reynolds Number was 730,000 for the model with the 0.20 c_w flap and 790,000 for the model with the 0.30 c_w flap. The flow conditions correspond approximately to those that would exist in free air at Reynolds Numbers of 1,000,000 and 1,100,000 respectively (reference 6).

Hinge moments of the flaps and ailerons were measured in the usual manner. A calibrated torque rod, attached to the surface under test and shielded from the air stream, was turned by a pointer mounted next to a graduated disk outside the jet. The difference of the pointer deflections required to bring the surface to the required deflection with the wind off and on was read from the disk. This difference is proportional to the aerodynamic moment about the hinge; the magnitude of the hinge moment follows directly from the known calibration of the rod.

The third phase of the investigation arose as the result of analysis of the data already obtained, which indicated that the ailerons would require excessive operating moments under certain conditions. It was therefore considered desirable to investigate the effectiveness of several methods of obtaining aileron balance. In order to reproduce ailerons of practical sizes with satisfactory accuracy, a special wide-chord model was constructed to be mounted between end planes. Although such an expedient does not reproduce full-scale conditions, practical aileron details, such as clearances and hinges, can be reproduced. As will subsequently be noted, leaks ahead of the aileron hinge resulting from clearance between the wing and the aileron have an appreciable effect on aileron characteristics and the clearance should therefore be accurately controlled.

The wide-chord model consisted of a rectangular N. A. C. A. 23012 airfoil having a chord of 4 feet and a span of 8 feet, equipped with an aileron of 31-inch span and 5.76-inch chord back of the hinge, located centrally along the span. The tests included the types of ailerons shown in figure 3: An ordinary aileron, an aileron with a nose balance shielded by curtains, an aileron with a Frise nose, and an aileron with a tab. An N. A. C. A. 23012 external-airfoil flap of 9.6-inch chord and 8-foot span was provided. The section of this model as tested was an accurate enlargement of that used for the standard-size model tested with the 0.20 c_w external-airfoil flap and 0.12 c_w ailerons. The model, complete with aileron and flap, was mounted between large end planes in the jet of the 7- by 10-foot tunnel. (See fig. 4.)

The regular force-test support, with two special struts for angle-of-attack adjustment, was used to permit measurement of the forces on the model. The aileron hinge moments were measured by a torque-rod and graduated-disk arrangement similar to that used for the standard-size model. Values of lift and drag increments due to aileron deflection and the variation of aileron hinge moment with deflection were measured

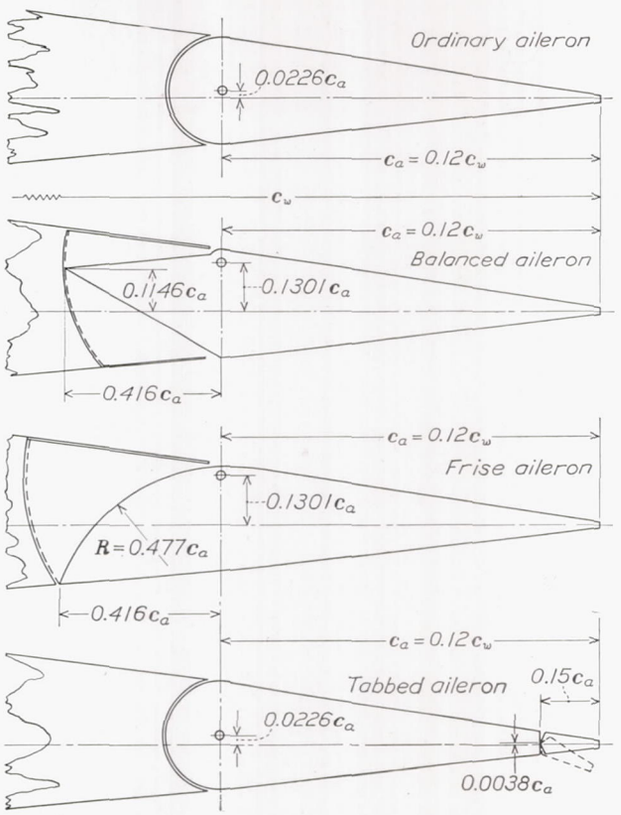

FIGURE 3.—Various balanced ailerons tested on the wide-chord N. A. C. A. 23012 airfoil with and without a 0.20 c_w N. A. C. A. 23012 external-airfoil flap.

at several angles of attack and flap angles. The tests were repeated with the flap removed to determine the effectiveness of the balancing means for narrow-chord ordinary ailerons mounted on a plain wing.

The tests of the wide-chord model were made, in general, at a dynamic pressure of 4.093 pounds per square foot, corresponding to an air speed of 40 miles per hour in standard air. The reduced speed was used to avoid placing excessive loads on the balance parts used as the model support. The effective Reynolds Number in this case was of the order of 5,000,000 but it should not be considered so accurate an index of flow similarity as is usually the case in wind-tunnel testing.

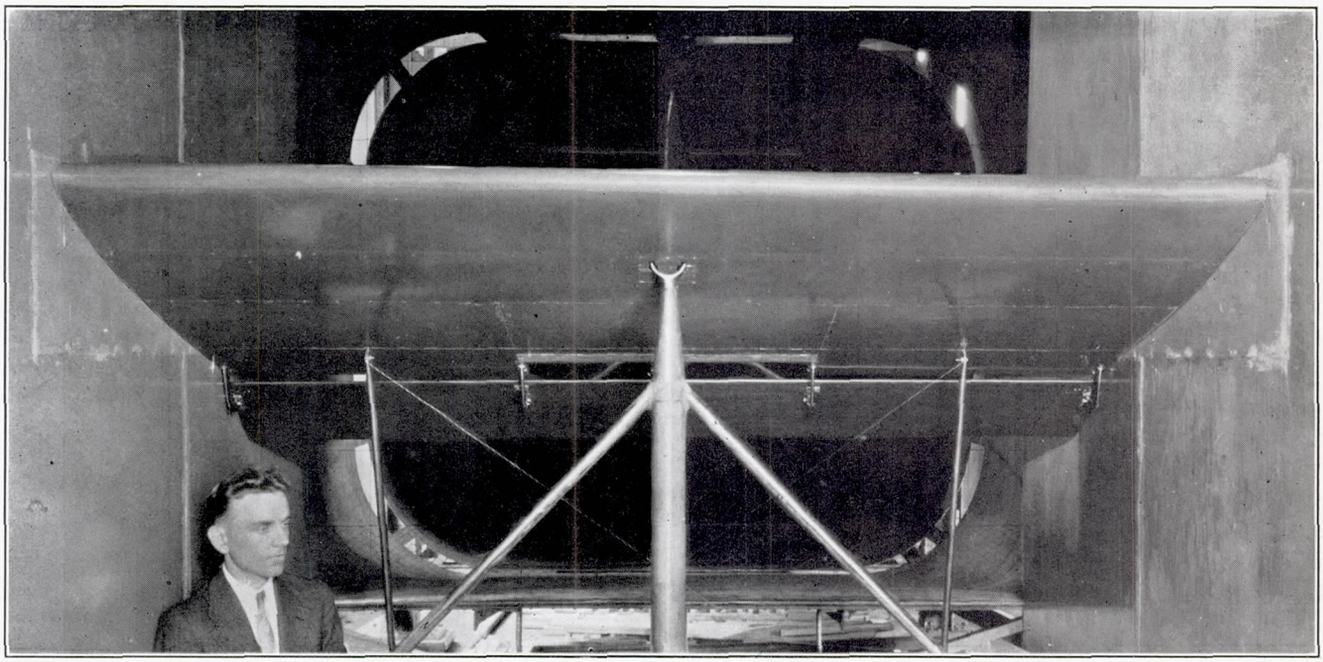

FIGURE 4.—The 4- by 8-foot model of the N. A. C. A. 23012 airfoil with an external-airfoil flap and an ordinary aileron, mounted between end planes in the 7- by 10-foot wind tunnel.

RESULTS

Application of results.—The precision of standard force tests in the 7- by 10-foot tunnel is discussed in references 2 and 5. The results as corrected are considered applicable to flight conditions with normal engineering accuracy at the previously stated values of the effective Reynolds Number. These values are too small to be directly usable in most cases but, with the aid of reference 7, a number of the characteristics of the present airfoils may be inferred for larger values of the Reynolds Number.

The conditions under which the ailerons on the wide-chord airfoil were tested were far removed from those for which theoretical wind-tunnel corrections may be applied; they therefore do not appear susceptible of accurate interpretation in terms of fundamental parameters. The ideal conditions in this respect were disregarded in favor of obtaining a reasonably accurate reproduction of the full-size ailerons themselves, including the end effects, to facilitate accurate comparison of the various ailerons tested. Consequently, any application to flight characteristics must be considered qualitative in nature. For comparison of the ailerons among themselves, however, the accuracy is probably much better than that usually obtained in standard small-scale tests, owing to the relatively large magnitude of the forces acting on the large model. The effectiveness of the data subsequently presented in showing consistent differences between the ailerons serves as an indication of the accuracy with which the values were measured.

Presentation and analysis of results.—The data obtained in the tests have been reduced to nondimensional coefficient form and are presented in a series of standard plots. The usual N. A. C. A. absolute coefficients are used throughout, except for a few symbols that have not been standardized. In the computation of the standard airfoil coefficients, the nominal area has been taken as the sum of the individual areas of the nonretracting surfaces (see references 2 and 4); the chord lengths have been similarly treated. The nonstandard coefficients are:

C_{n_i}, induced yawing-moment coefficient.

C_{n_0}, profile yawing-moment coefficient.

C_h, hinge-moment coefficient based on the dimensions of the surface whose hinge moment is being measured. $\left(\text{Thus, } C_{h_f}=\frac{H_f}{c_f S_f q}\right)$

ΔC_L, the increment of lift coefficient produced by a specified deflection of the aileron on the wide-chord model.

ΔC_D, the increment of drag corresponding to ΔC_L.

δ, angular deflection of the chord line of an auxiliary surface from the chord line of the surface to which it is attached, having the same sign convention as angle of attack.

The following subscripts serve to identify the various parts of the complete wing model:

w, of the main airfoil.

f, of the flap.

a, of the aileron.

t, of the tab.

The results of the first phase of the investigation consist entirely of lift, drag, pitching-moment, and flap hinge-moment data relating to the two high-lift arrangements tested. Data for the plain N. A. C. A. 23012 airfoil used as the basic airfoil are shown in figure 5 together with data from another airfoil of the same section. The data for the basic airfoil equipped with a 0.20 c_w N. A. C. A. 23012 external-airfoil flap deflected through various angles appear in figures 6 to 9.

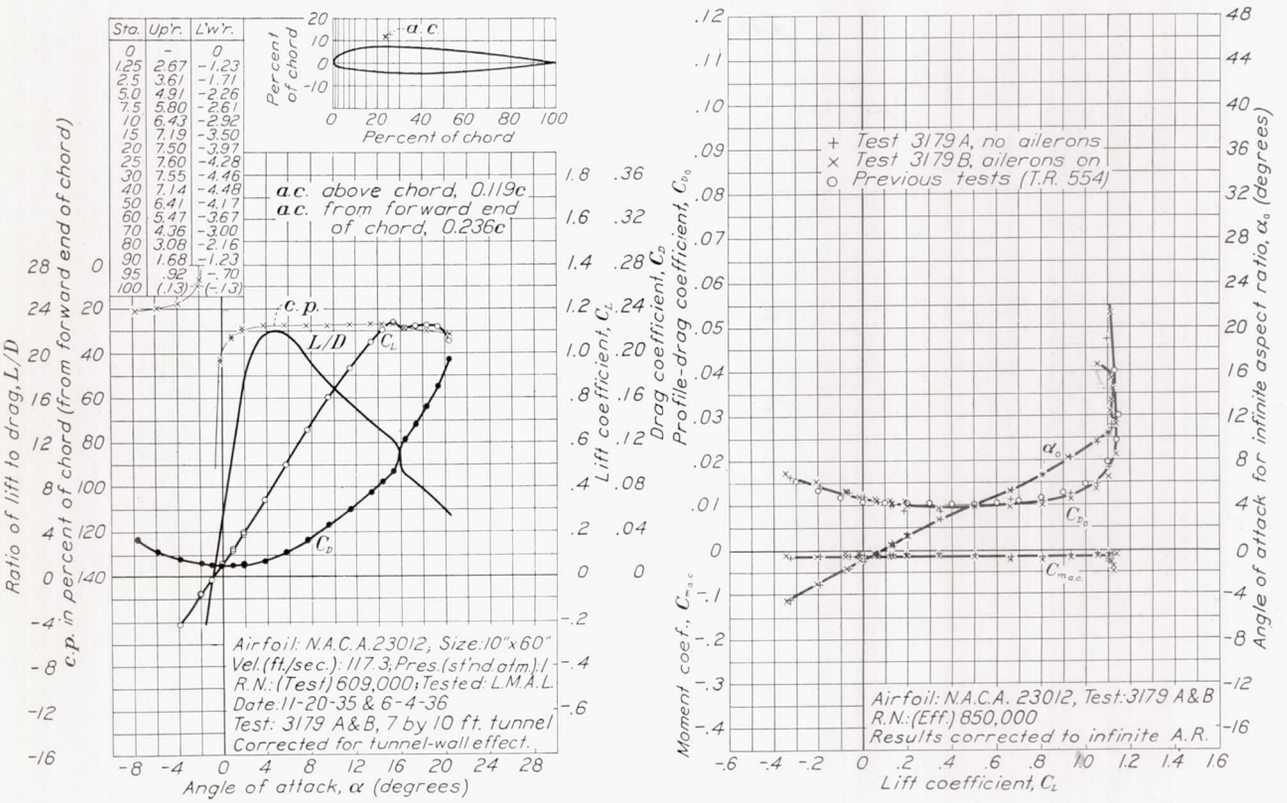

FIGURE 5.—The N. A. C. A. 23012 airfoil.

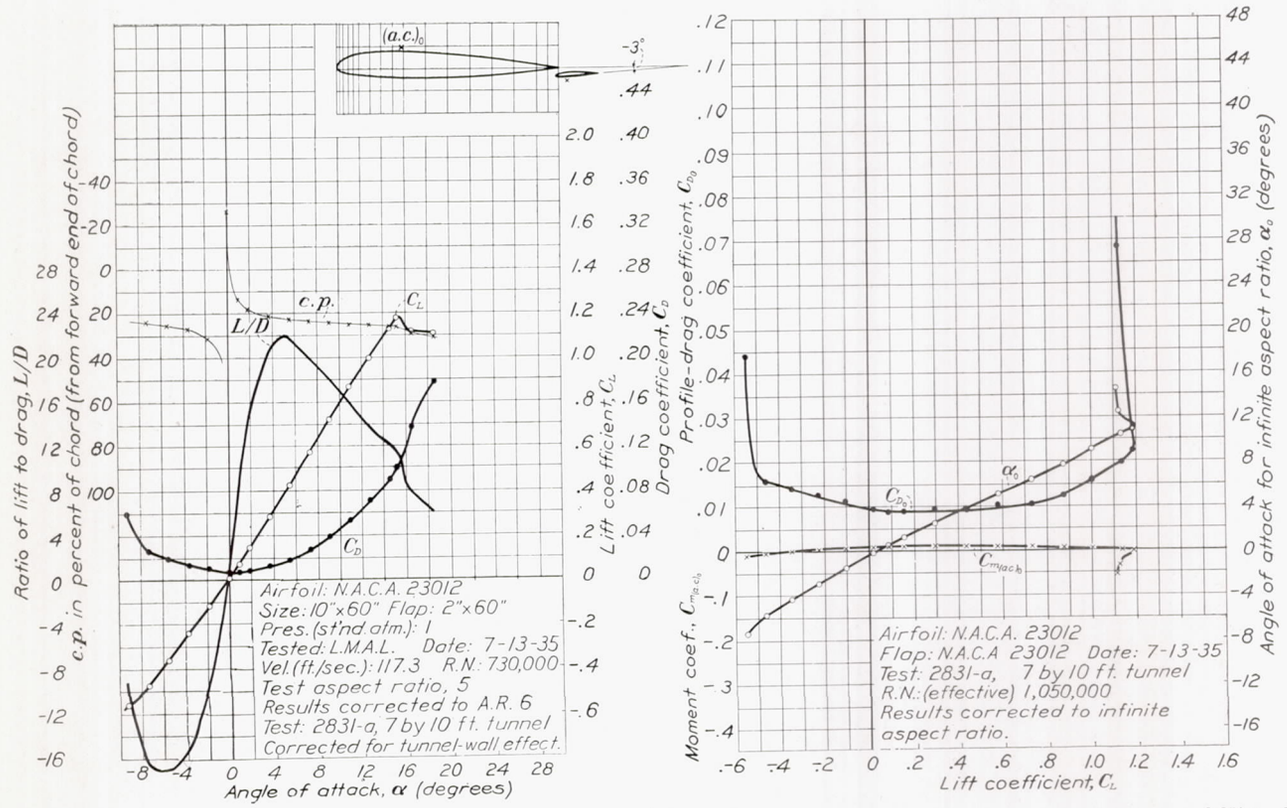

Main wing section	N. A. C. A. 23012	
Flap section	N. A. C. A. 23012	
Main wing chord, c_w	0.833 c	
Flap chord, c_f	0.20 c_w	.1667 c
Datum chord, $c=c_w+c_f$.		
Pivot aft of trailing edge of c_w	.032 c_w	.0266 c
Pivot below c_w	0.054 c_w	0.045 c
Pivot aft of flap leading edge	.25 c_f	.0417 c
Pivot below c_f	.10 c_f	.0167 c
Flap displacement angle		−3°
$(a.c.)_0$ from leading edge		.245 c
$(a.c.)_0$ above main wing chord		.08 c

FIGURE 6.—The N. A. C. A. 23012 airfoil with 0.20 c_w N. A. C. A. external-airfoil flap. Flap angle, −3°. (See reference 4.)

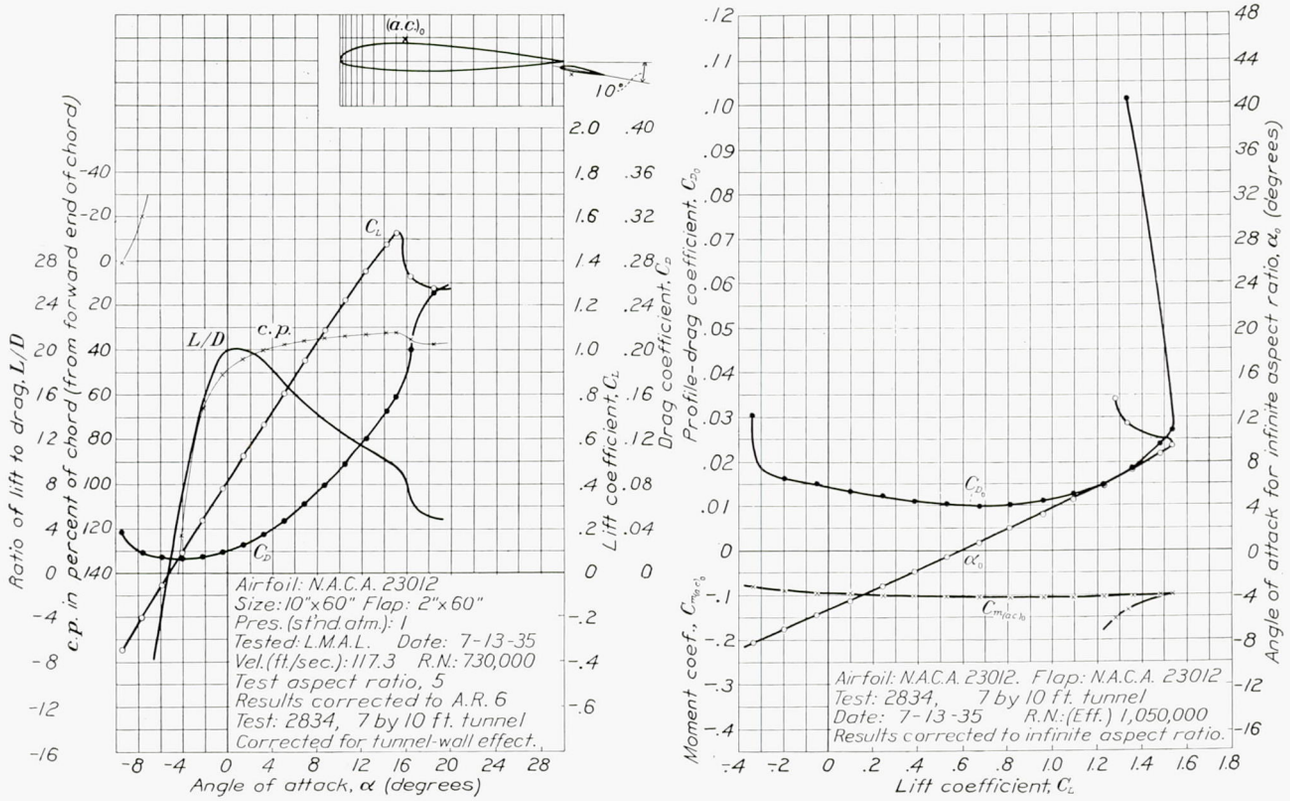

FIGURE 7.—The N. A. C. A. 23012 airfoil with 0.20 c_w N. A. C. A. external-airfoil flap. Flap angle, 10°. The airfoil is the same as used for test 2831-a (fig. 6), except the flap setting. The value of $C_{m\,(a.c.)_0}$ is computed about the aerodynamic center used for test 2831-a. (See reference 4.)

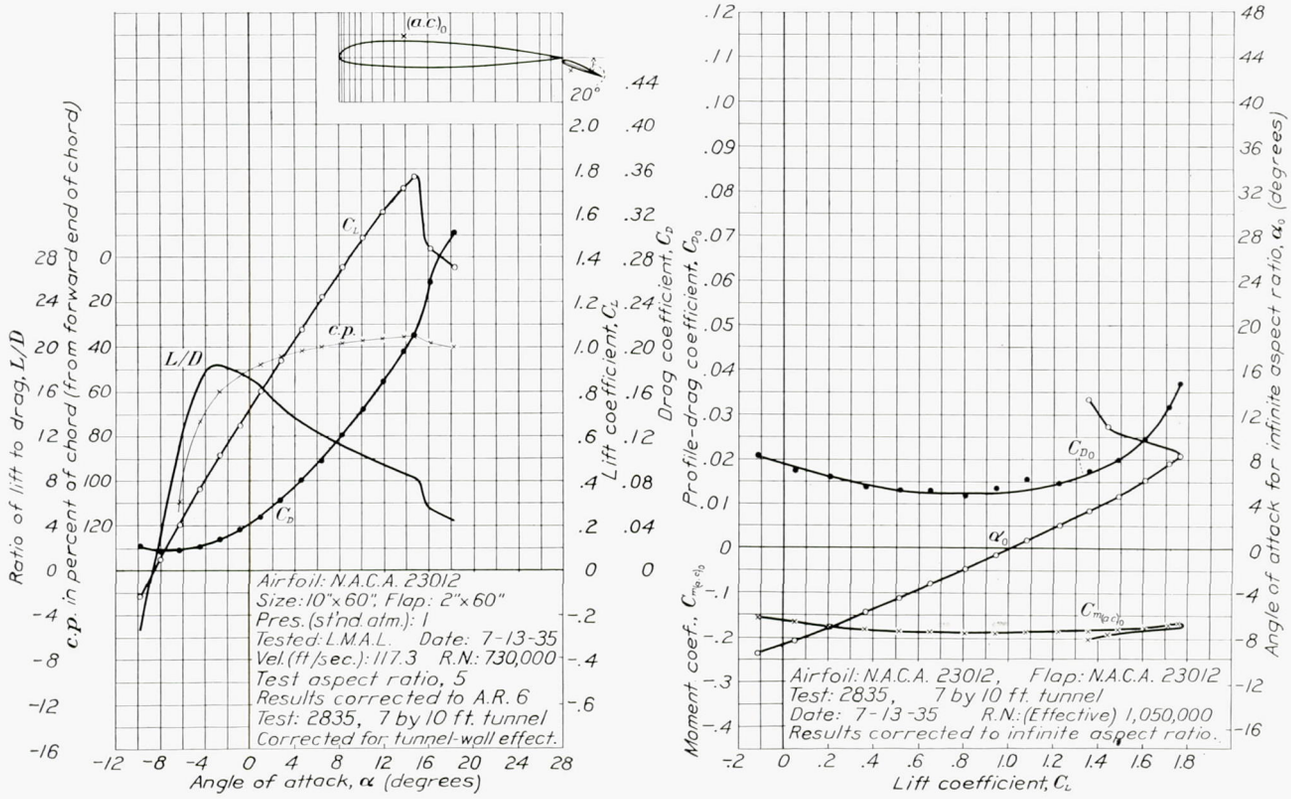

FIGURE 8.—The N. A. C. A. 23012 airfoil with 0.20 c_w N. A. C. A. 23012 external-airfoil flap. Flap angle 20°. The airfoil is the same as used for test 2831-a (fig. 6), except the flap setting. The value of $C_{m\,(a.c.)_0}$ is computed about the aerodynamic center used for test 2831-a. (See reference 4.)

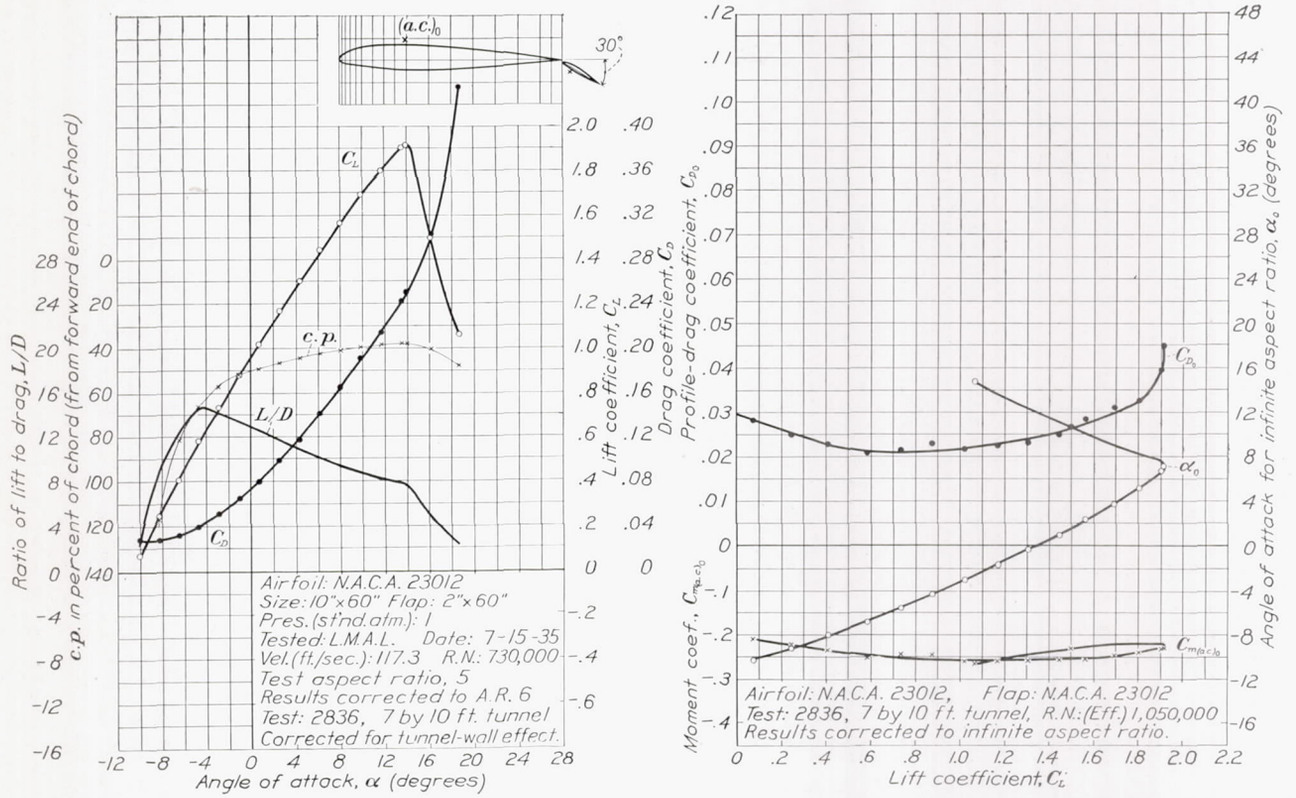

FIGURE 9.—The N. A. C. A. 23012 airfoil with 0.20 c_w N. A. C. A. 23012 external-airfoil flap. Flap angle, 30°. The airfoil is the same as used for test 2831–a (fig. 6), except the flap setting. The value of $C_{m_{(a.c.)_0}}$ is computed about the aerodynamic center used for test 2831–a. (See reference 4.)

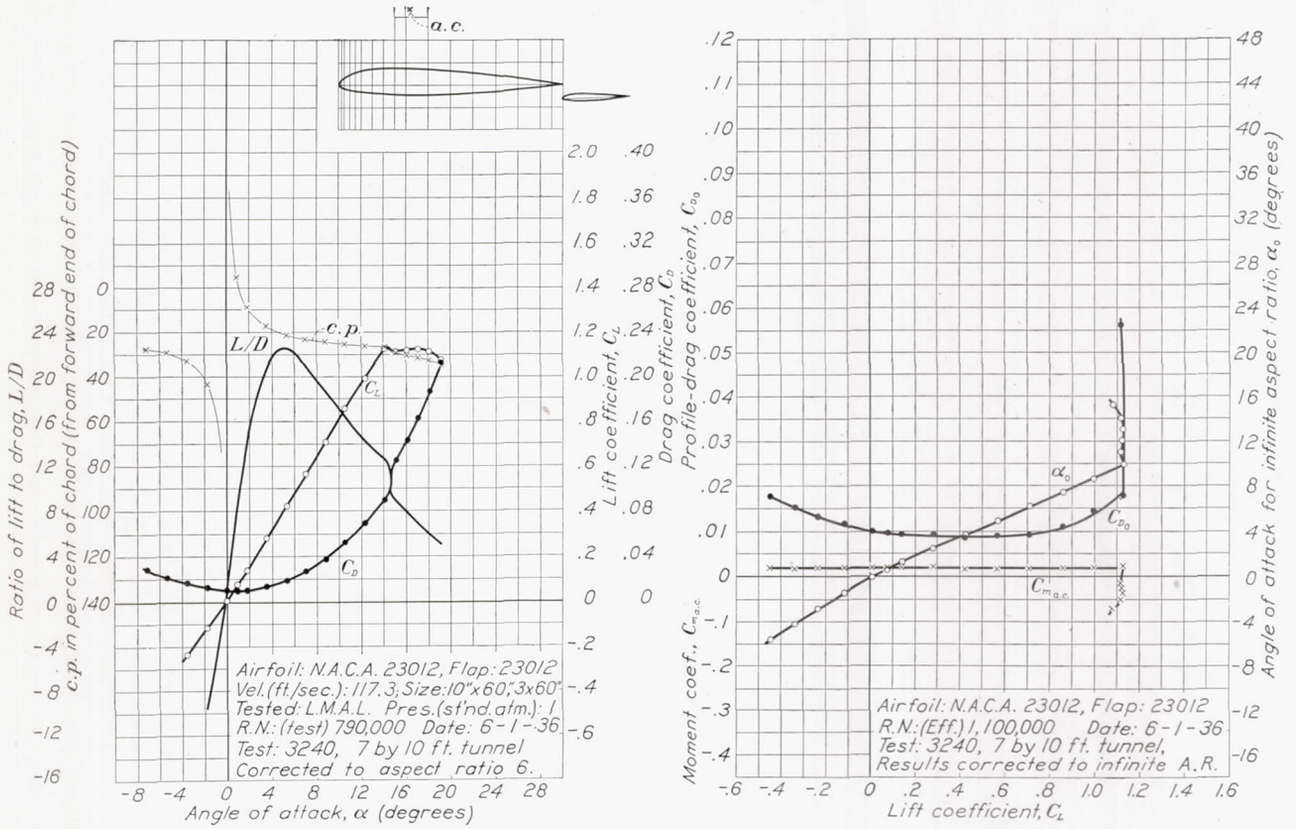

Main wing section	N. A. C. A. 23012	
Flap section	N. A. C. A. 23012	
Over-all wing chord, $c=c_w+c_f$.		
Main wing chord, c_w		0.769 c
Flap chord, c_f	0.30 c_w	.231 c
Datum chord, $c=c_w+c_f$.		

Pivot aft of trailing edge of c_w	0.071 c_w	0.0546 c
Pivot below c_w	.049 c_w	.0377 c
Pivot aft of flap leading edge	.25 c_f	.0577 c
Flap displacement angle		−2°
$a.c.$ from leading edge		.246 c
$a.c.$ above main wing chord		.260 c

FIGURE 10.—The N. A. C. A. 23012 airfoil with 0.30 c_w N. A. C. A. 23012 external-airfoil flap. Flap angle, −2°.

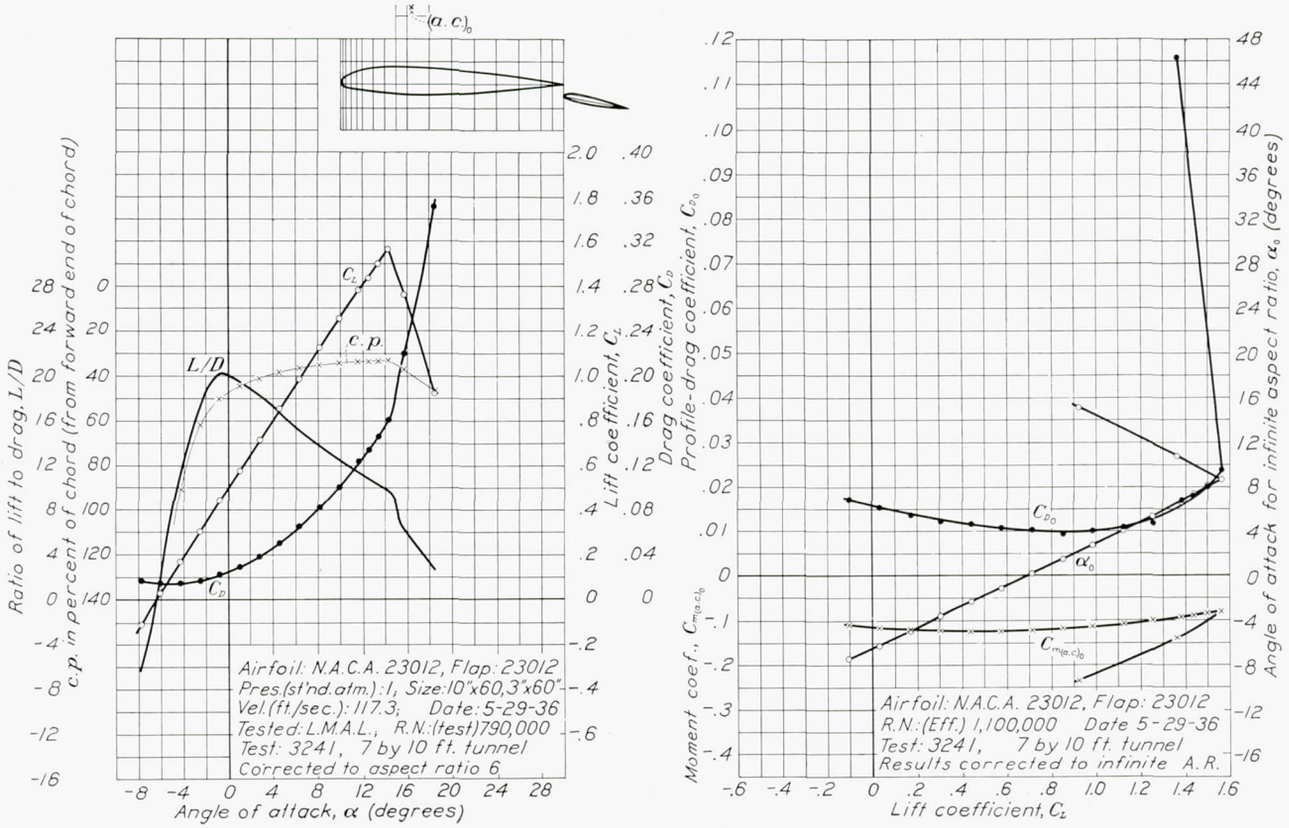

FIGURE 11.—The N. A. C. A. 23012 airfoil with 0.30 c_w N. A. C. A. 23012 external-airfoil flap. Flap angle, 10°. The airfoil is the same as used for test 3240 (fig. 10), except the flap setting. The value of $C_{m\,(a.c.)_0}$ is computed about the aerodynamic center used for test 3240.

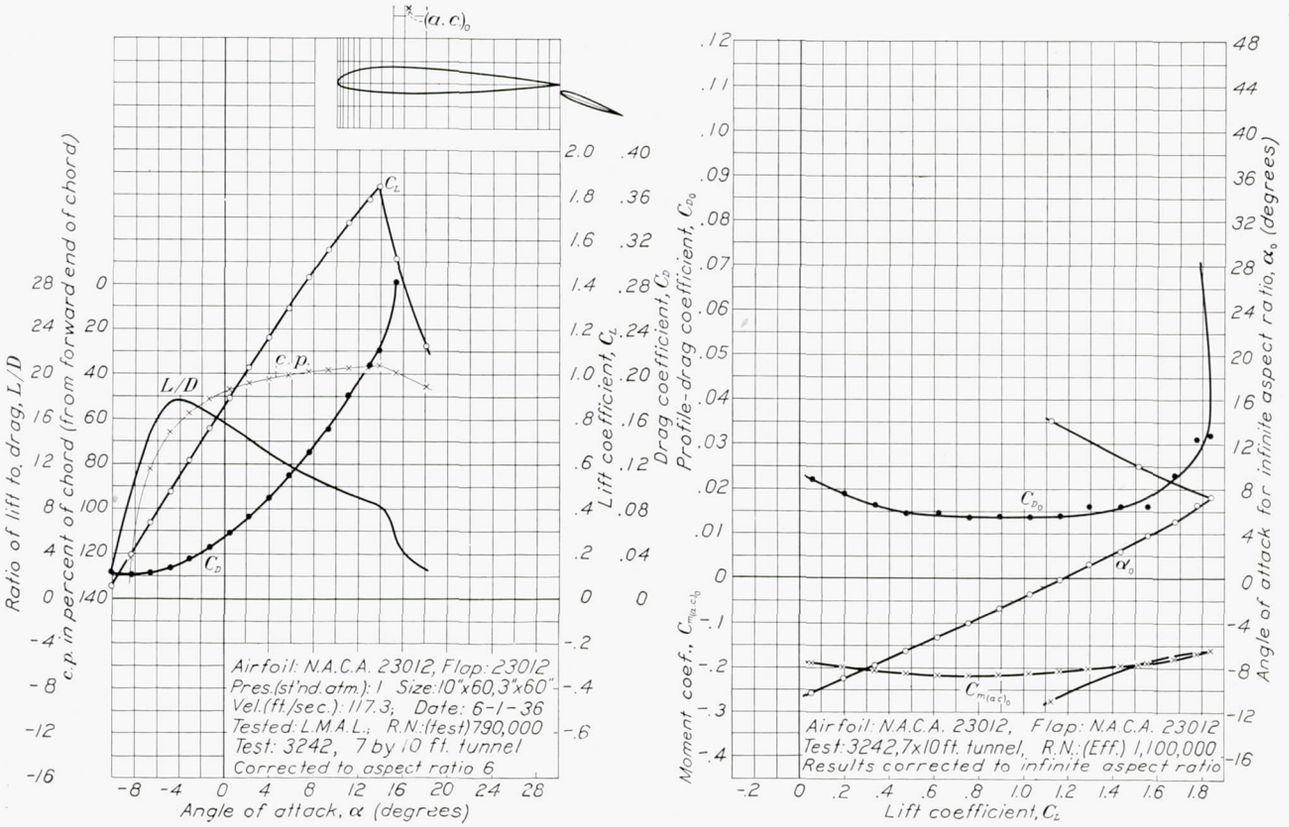

FIGURE 12.—The N. A. C. A. 23012 airfoil with 0.30 c_w N. A. C. A. 23012 external-airfoil flap. Flap angle, 20°. The airfoil is the same as used for test 3240 (fig. 10), except the flap setting. The value of $C_{m\,(a.c.)_0}$ is computed about the aerodynamic center used for test 3240.

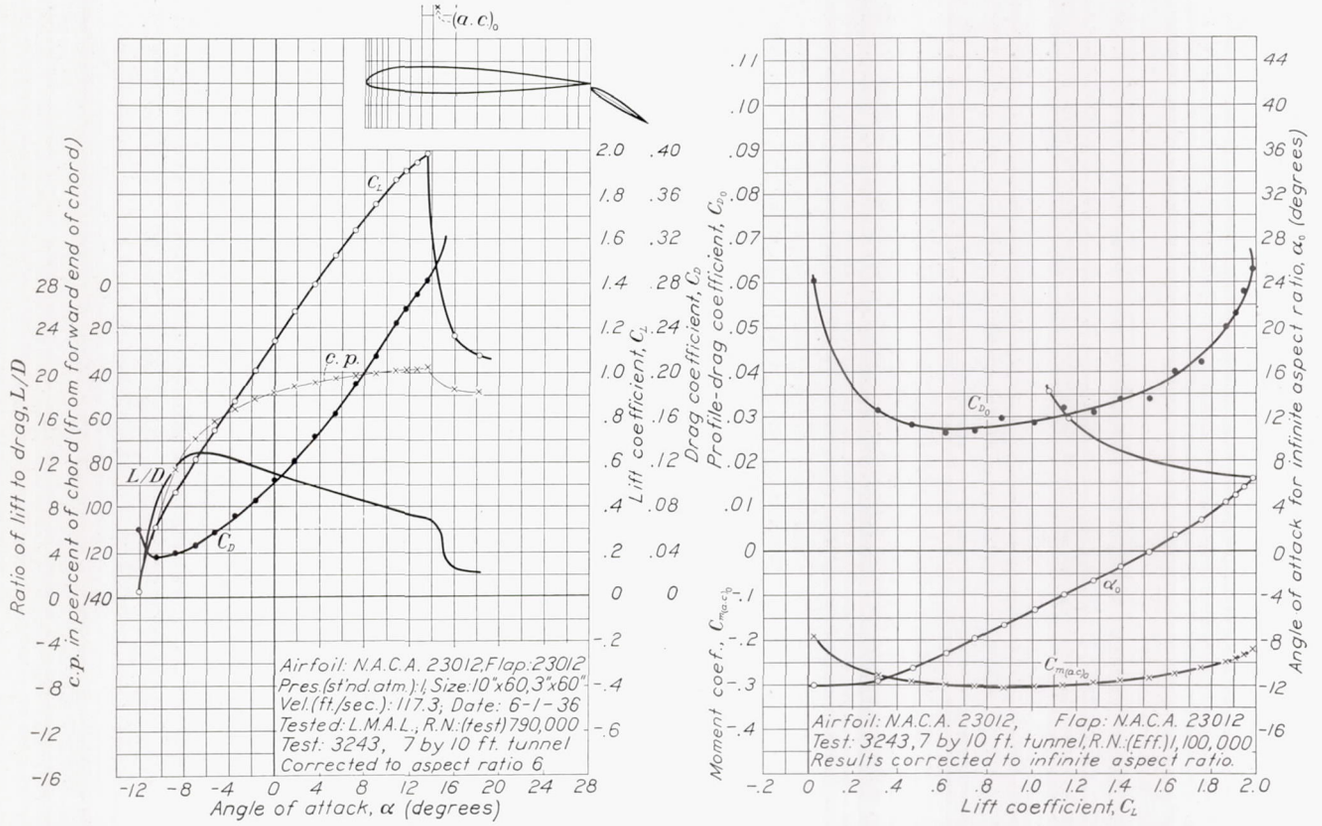

FIGURE 13.—The N. A. C. A. 23012 airfoil with 0.30 c_w N. A. C. A. 23012 external-airfoil flap. Flap angle, 30°. The airfoil is the same as used for test 3240 (fig. 10), except the flap setting. The value of $C_{m\,(a.c.)_0}$ is computed about the aerodynamic center used for test 3240.

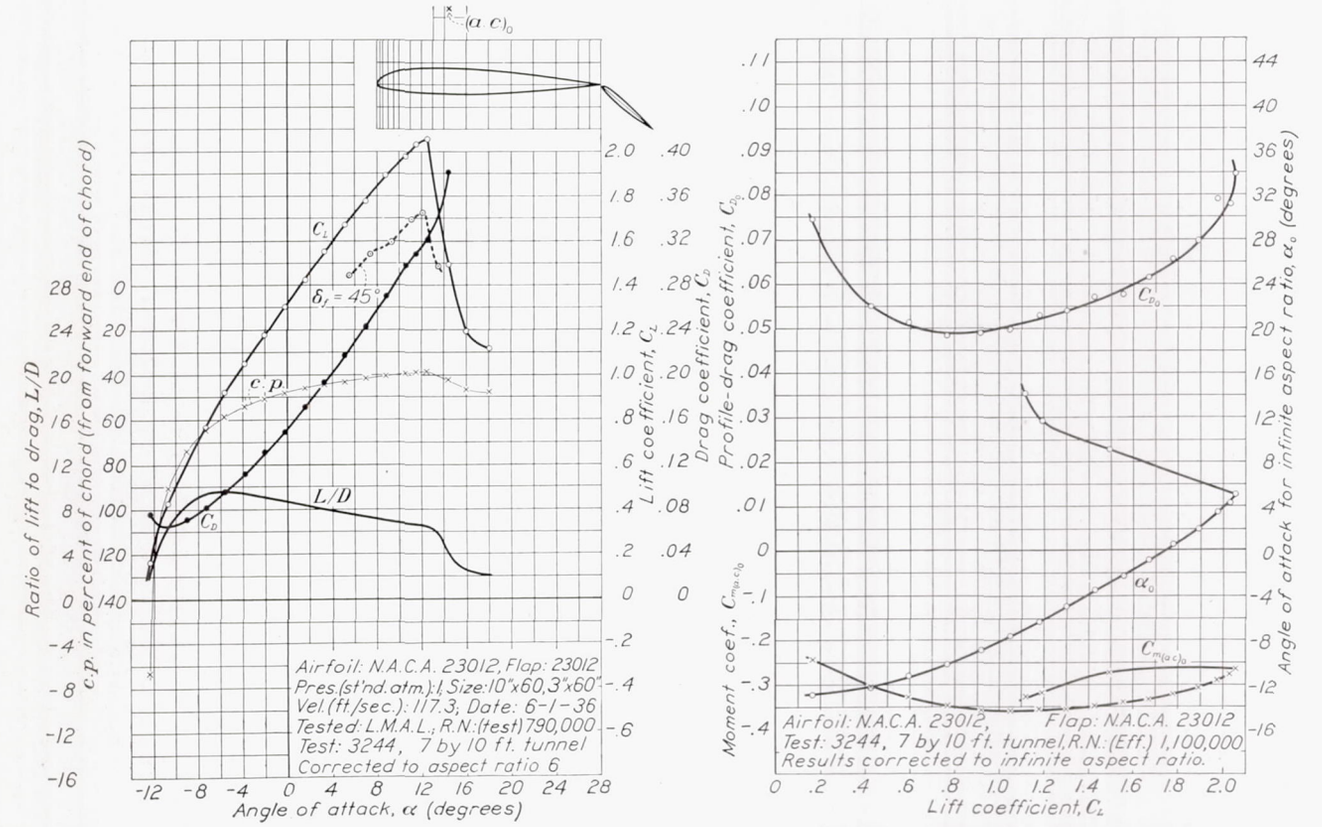

FIGURE 14.—The N. A. C. A. 23012 airfoil with 0.30 c_w N. A. C. A. 23012 external-airfoil flap. Flap angle, 40°. The airfoil is the same as used for test 3240 (fig. 10), except the flap setting. The value of $C_{m\,(a.c.)_0}$ is computed about the aerodynamic center used for test 3240.

The data for the basic airfoil equipped with a 0.30 c_w external-airfoil flap of N. A. C. A. 23012 section appear in figures 10 to 14. The variation of flap hinge-moment coefficient with flap angle and angle of attack for each flap is shown in figure 15. It will be noted that the geometric aspect ratios of the model with the 0.20 c_w and 0.30 c_w flaps were 5.0 and 4.61, respectively. For purposes of comparison the data have been corrected in the usual manner (reference 2) for jet-boundary and planform effects and are presented in the standard airfoil plots for aspect ratios of 6 and infinity. Likewise, the angles of attack shown for the flap hinge-moment coefficient plots (fig. 15) refer to the conditions for a wing of aspect ratio 6 in an infinite jet.

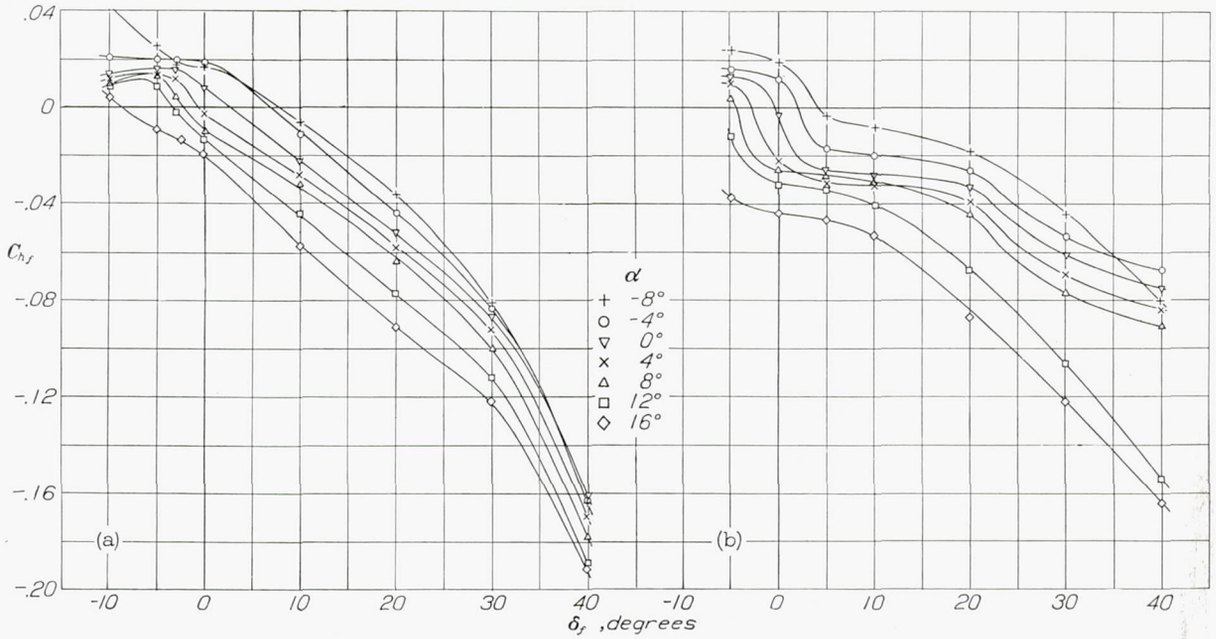

(a) The N. A. C. A. 23012 airfoil with 0.20 c_w external-airfoil flap. (b) The N. A. C. A. 23012 airfoil with 0.30 c_w external-airfoil flap.

FIGURE 15.—Variation of flap hinge-moment coefficient with flap deflection, at several angles of attack.

The results of the second phase of the investigation consist of rolling-moment, yawing-moment, and hinge-moment coefficients, presented as functions of angular deflection of the right aileron, the left aileron being held neutral. The data for the basic model equipped with the 0.20 c_w external-airfoil flap and the 0.12 c_w ailerons appear in figures 16 to 19; those for the model with the 0.30 c_w external-airfoil flap and 0.13 c_w ailerons in figures 20 to 23. For purposes of comparison the rolling- and yawing-moment coefficients have been corrected for jet-boundary and aspect-ratio effects so that the data as presented are representative of conditions existing on a model of aspect ratio 6 in an infinite jet. The method employed in making the corrections is explained in an appendix to this report. Since the effect of jet boundaries on measured rolling-moment coefficients is neglected, the plotted values are directly comparable with those obtained in previous lateral-control investigations in the 7- by 10-foot tunnel. The magnitude of the jet-boundary correction of yawing moment is normally small, and the present results may, therefore, be roughly compared with data obtained in previous investigations without correction. For accurate comparison of yawing-moment data, however, previous results should be corrected for the effect of the jet boundaries on induced yawing moment by the method given in the appendix.

The data in the figures have been selected from cross-fairings against angle of attack in such a way as to show the lateral-control characteristics at angles of attack corresponding to lift coefficients of 0.2, 0.7, 1.2, and 1.8 with the ailerons neutral. The variation of lift coefficient with aileron deflection at a given angle of attack was neglected. The lift coefficients were selected as representative of certain flight conditions: high speed, maximum rate of climb, steep climb and approach glide, and flight immediately before landing and after take-off.

The plots of yawing-moment coefficient against rolling-moment coefficient may be regarded as analogous to polar curves of lift and drag. As indicated in the appendix, the theoretical induced yawing-moment coefficients are shown in the figures. By this artifice the figures are made to show the induced and profile parts into which the measured yawing moment may be divided.

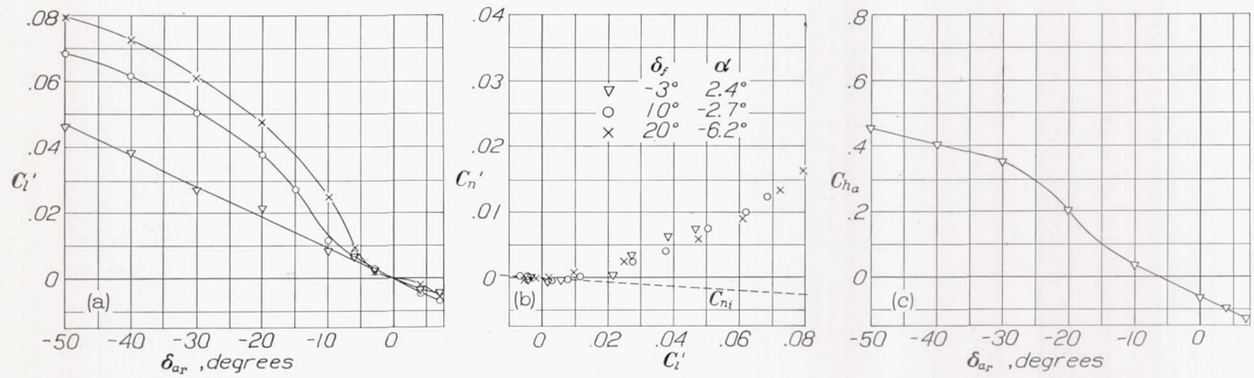

(a) Variation of rolling-moment coefficient with deflection of right aileron. Left aileron, 0°.

(b) Variation of yawing-moment coefficient with rolling-moment coefficient.

(c) Variation of aileron hinge-moment coefficient with aileron deflection.

FIGURE 16.—Rolling-, yawing-, and hinge-moment coefficients of N. A. C. A. 23012 airfoil with 0.12 c_w ordinary aileron and 0.20 c_w external-airfoil flap. C_L=0.2.

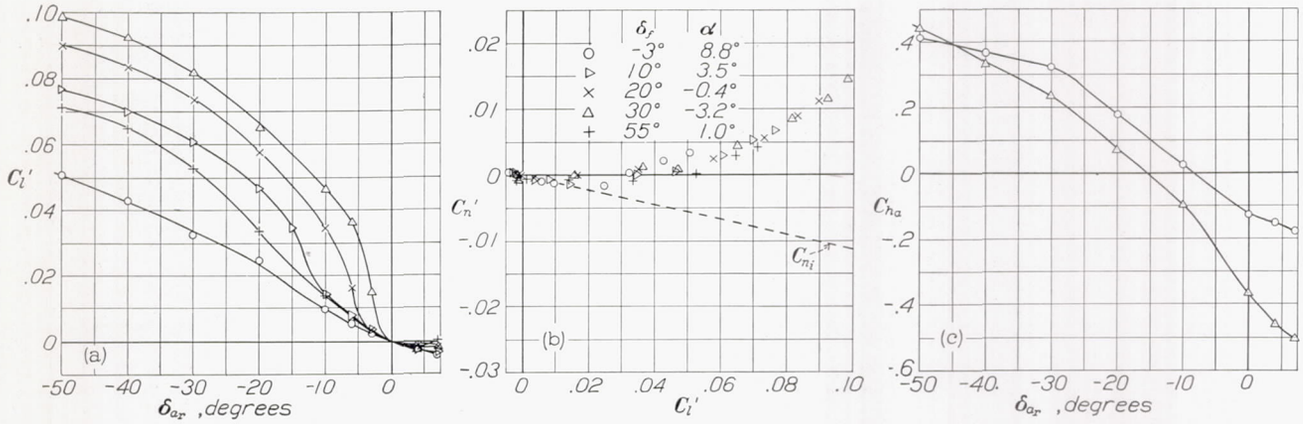

(a) Variation of rolling-moment coefficient with deflection of right aileron. Left aileron, 0°.

(b) Variation of yawing-moment coefficient with rolling-moment coefficient.

(c) Variation of aileron hinge-moment coefficient with aileron deflection.

FIGURE 17.—Rolling-, yawing-, and hinge-moment coefficients of N. A. C. A. 23012 airfoil with 0.12 c_w ordinary aileron and 0.20 c_w external-airfoil flap. C_L=0.7.

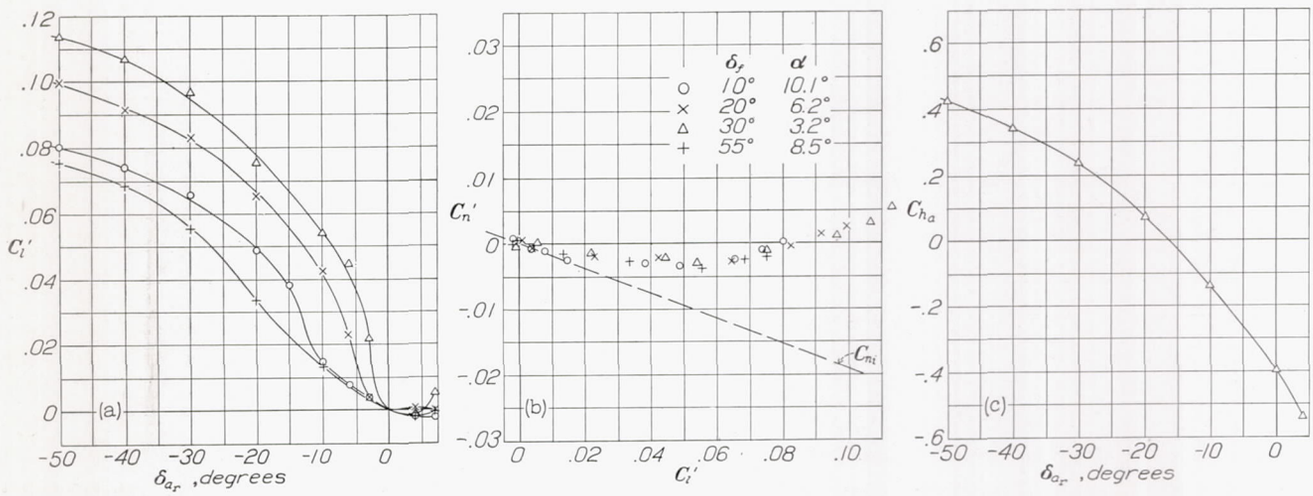

(a) Variation of rolling-moment coefficient with deflection of right aileron. Left aileron, 0°.

(b) Variation of yawing-moment coefficient with rolling-moment coefficient.

(c) Variation of aileron hinge-moment coefficient with aileron deflection.

FIGURE 18.—Rolling-, yawing-, and hinge-moment coefficients of N. A. C. A. 23012 airfoil with 0.12 c_w ordinary aileron and 0.20 c_w external-airfoil flap. C_L=1.2.

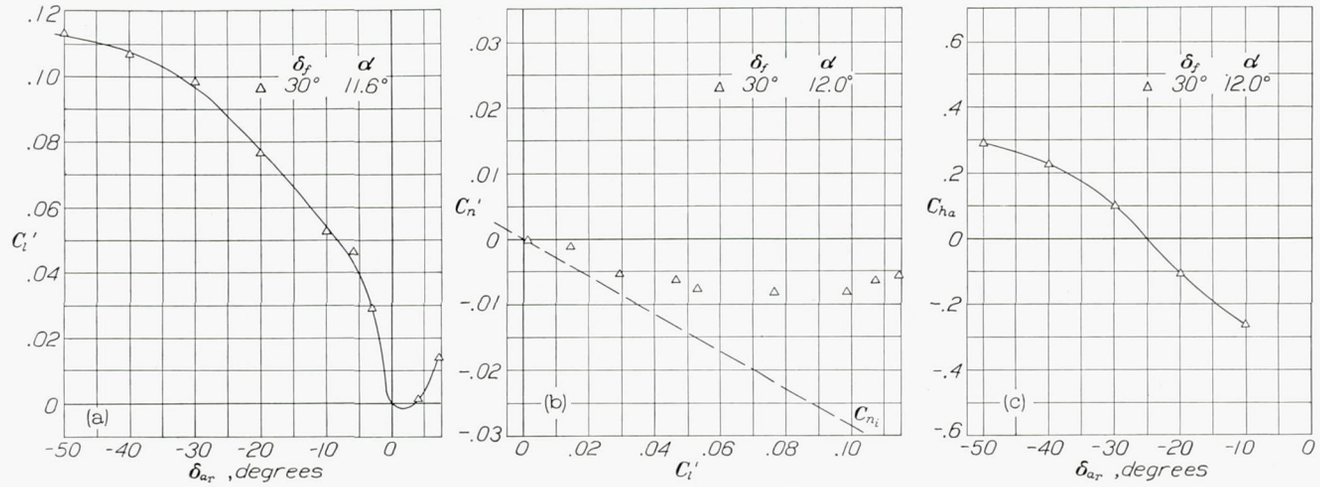

(a) Variation of rolling-moment coefficient with deflection of right aileron. Left aileron, 0°.

(b) Variation of yawing-moment coefficient with rolling-moment coefficient.

(c) Variation of aileron hinge-moment coefficient with aileron deflection.

FIGURE 19.—Rolling-, yawing-, and hinge-moment coefficients of N. A. C. A. 23012 airfoil with 0.12 c_w ordinary aileron and 0.20 c_w external-airfoil flap. C_L=1.8.

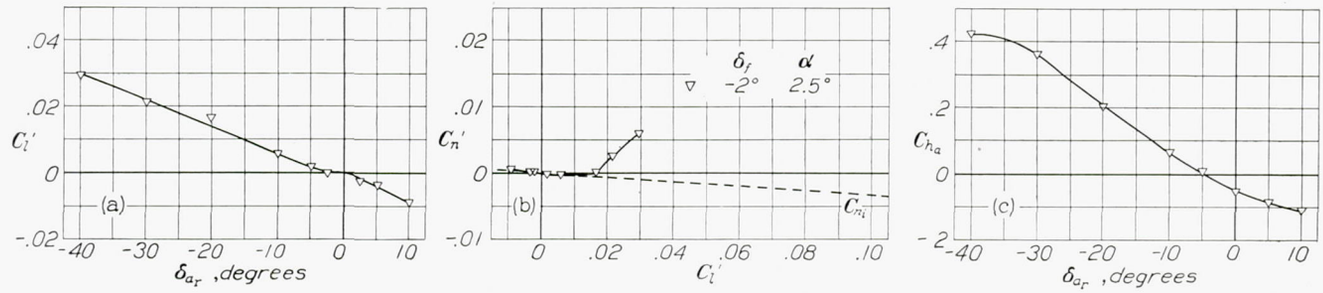

(a) Variation of rolling-moment coefficient with deflection of right aileron. Left aileron, 0°.

(b) Variation of yawing-moment coefficient with rolling-moment coefficient.

(c) Variation of aileron hinge-moment coefficient with aileron deflection.

FIGURE 20.—Rolling-, yawing-, and hinge-moment coefficient of N. A. C. A. 23012 airfoil with 0.13 c_w ordinary aileron and 0.30 c_w external-airfoil flap. C_L=0.2.

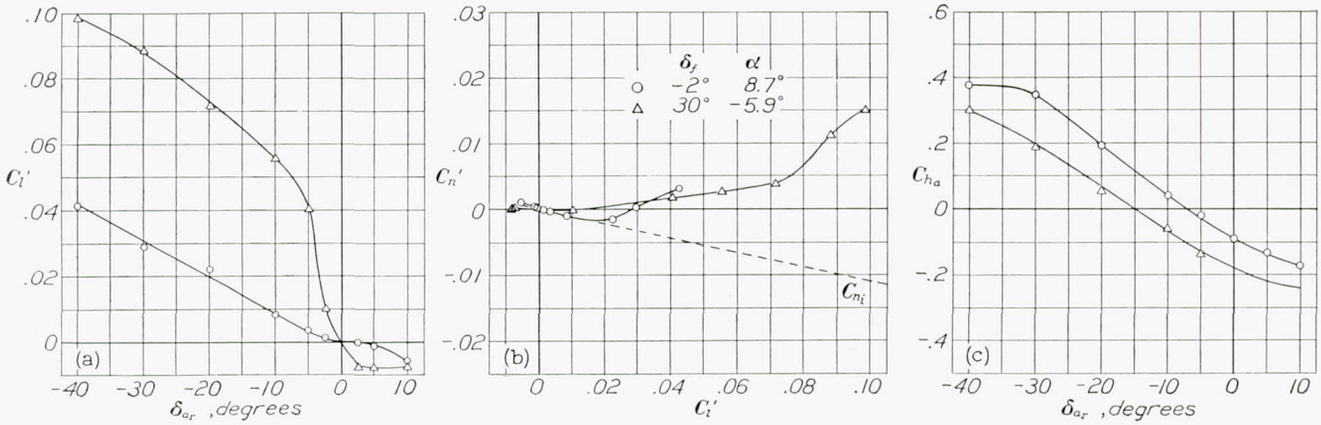

(a) Variation of rolling-moment coefficient with deflection of right aileron. Left aileron, 0°.

(b) Variation of yawing-moment coefficient with rolling-moment coefficient.

(c) Variation of aileron hinge-moment coefficient with aileron deflection.

FIGURE 21.—Rolling-, yawing-, and hinge-moment coefficients of N. A. C. A. 23012 airfoil with 0.13 c_w ordinary aileron and 0.30 c_w external-airfoil flap. C_L=0.7.

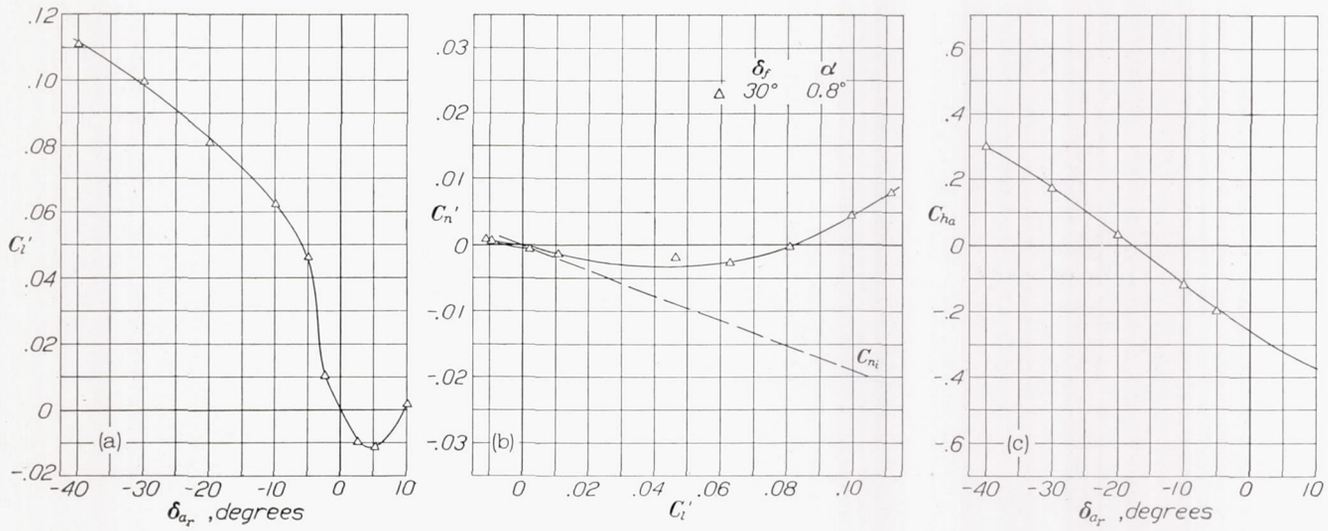

(a) Variation of rolling-moment coefficient with deflection of right aileron. Left aileron, 0°.

(b) Variation of yawing-moment coefficient with rolling-moment coefficient.

(c) Variation of aileron hinge-moment coefficient with aileron deflection.

FIGURE 22.—Rolling-, yawing-, and hinge-moment coefficients of N. A. C. A. 23012 airfoil with 0.13 c_w ordinary aileron and 0.30 c_w external-airfoil flap. C_L=1.2.

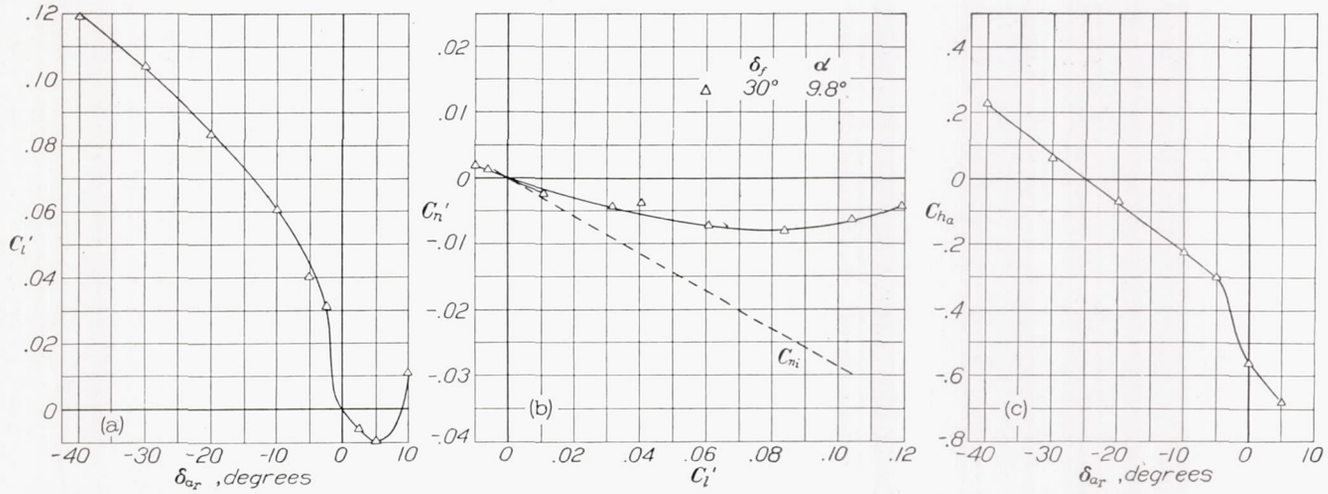

(a) Variation of rolling-moment coefficient with deflection of right aileron. Left aileron, 0°.

(b) Variation of yawing-moment coefficient with rolling-moment coefficient.

(c) Variation of aileron hinge-moment coefficient with aileron deflection.

FIGURE 23.—Rolling-, yawing-, and hinge-moment coefficients of N. A. C. A. 23012 airfoil with 0.13 c_w ordinary aileron and 0.30 c_w external-airfoil flap. C_L=1.8.

The data obtained in the third phase of the investigation are given in figures 24 to 31. The measured values of lift and drag have been reduced to the form of the lift and drag increments that result from a given deflection of the aileron under test. The lift increment produced by a deflected aileron on an airplane wing is the direct source of the rolling moment obtained; the drag increment likewise produces a corresponding yawing moment. Thus, under comparable conditions of wing lift coefficient and flap setting, the rolling and yawing moments that one of the ailerons under test would produce on an airplane wing are directly proportional to the measured lift and drag increments. The factor of proportionality varies with wing plan form but, for a given plan form, the factor remains constant regardless of aileron deflection. The curves of lift increment against aileron deflection and drag increment against lift increment are therefore analogous in form to the rolling- and yawing-moment data previously presented. Absolute values of hinge moment as a function of aileron deflection are also given—these values are directly comparable with the data obtained for the standard model.

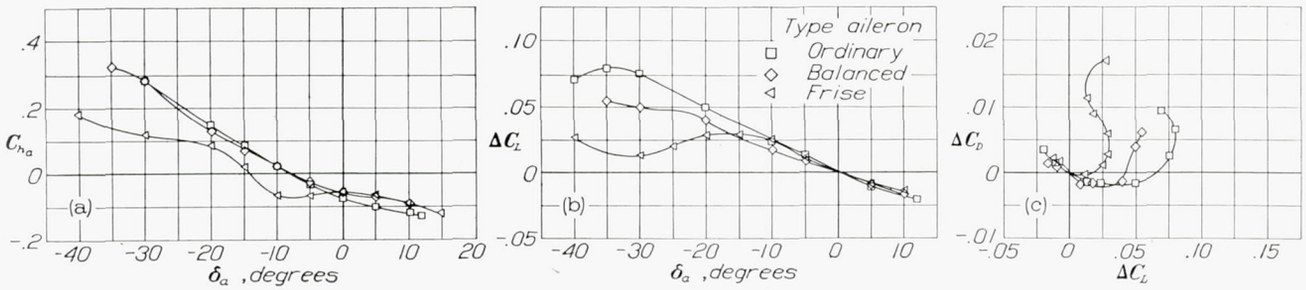

(a) Variation of aileron hinge-moment coefficient with aileron deflection.

(b) Variation of lift-coefficient increment with aileron deflection.

(c) Variation of drag-coefficient increment with lift-coefficient increment.

FIGURE 24.—Characteristics of various balanced ailerons on N. A. C. A. 23012 airfoil with 0.20 c_w external-airfoil flap set at −3°. C_L=0.2.

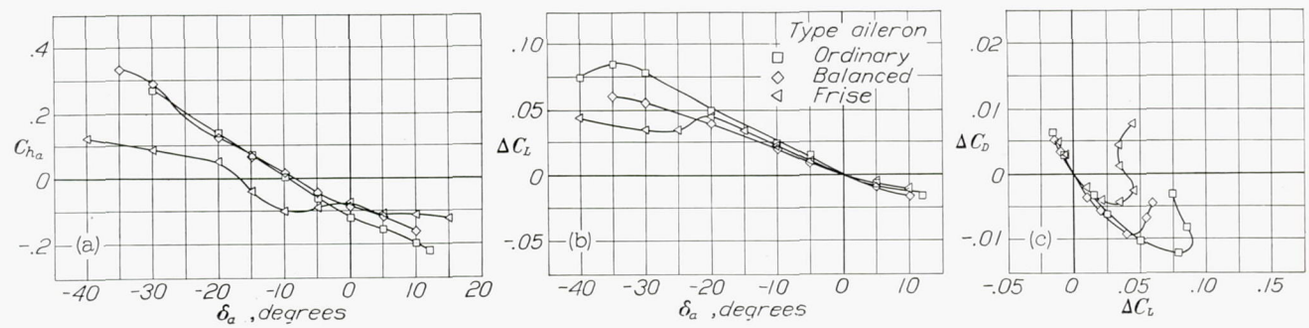

(a) Variation of aileron hinge-moment coefficient with aileron deflection.

(b) Variation of lift-coefficient increment with aileron deflection.

(c) Variation of drag-coefficient increment with lift-coefficient increment.

FIGURE 25.—Characteristics of various balanced ailerons on N. A. C. A. 23012 airfoil with 0.20 c_w external-airfoil flap set at −3°. C_L=0.7.

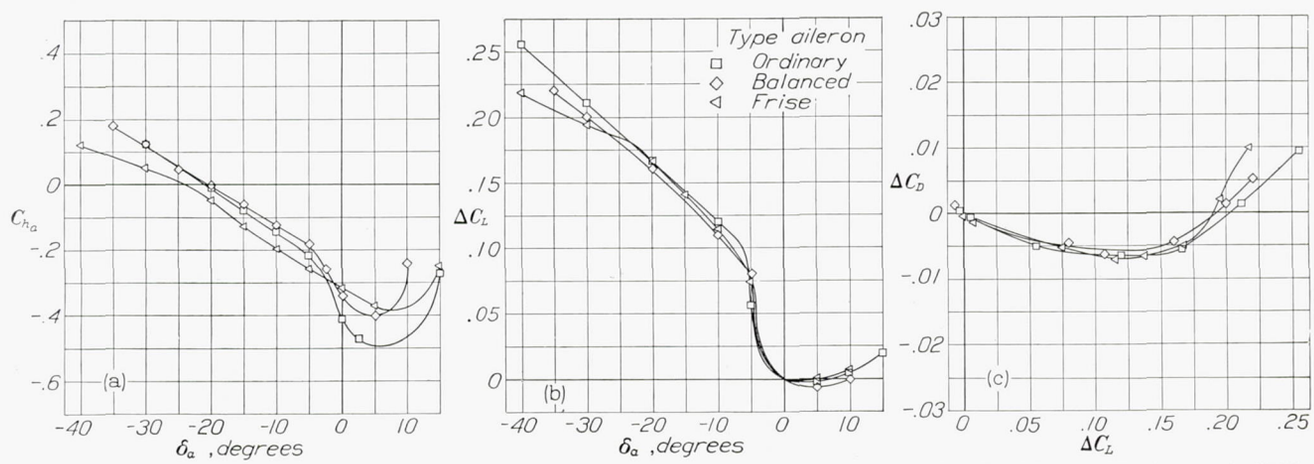

(a) Variation of aileron hinge-moment coefficient with aileron deflection.

(b) Variation of lift-coefficient increment with aileron deflection.

(c) Variation of drag-coefficient increment with lift-coefficient increment.

FIGURE 26.—Characteristics of various balanced ailerons on N. A. C. A. 23012 airfoil with 0.20 c_w external-airfoil flap set at 25°. C_L=0.7.

The data for the wide-chord model with the flap and each of the first three ailerons tested (that is, the plain aileron, the balanced aileron, and the Frise aileron) have been cross-faired to obtain the values of the variables at the same values of lift coefficient that were used for the previous figures and are plotted in figures 24 to 27. Similar data for the model with the same three ailerons but without the flap are shown in figures 28 and 29.

No lift and drag measurements were made of the model with the tabbed aileron because it could be assumed that the aileron lift and drag increments at small constant tab deflections were the same as those for the ordinary aileron without a tab. Experience coincides with flap theory in justifying this assumption for the unstalled lift range although it cannot be expected to hold at lift coefficients very near the stall.

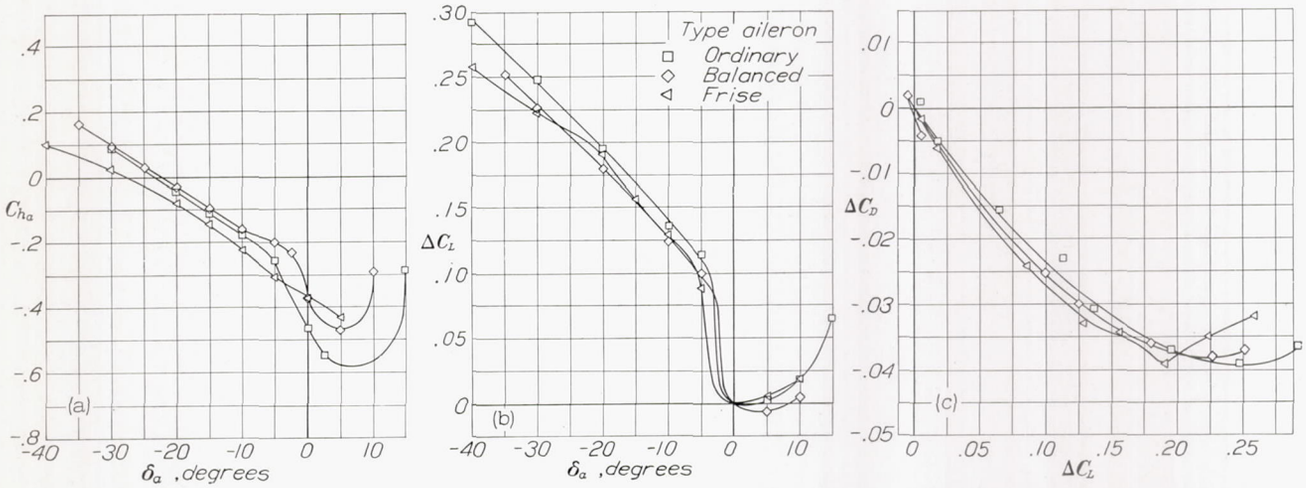

(a) Variation of aileron hinge-moment coefficient with aileron deflection.

(b) Variation of lift-coefficient increment with aileron deflection.

(c) Variation of drag-coefficient increment with lift-coefficient increment.

FIGURE 27.—Characteristics of various balanced ailerons on N. A. C. A. 23012 airfoil with 0.20 c_w external-airfoil flap set at 25°. C_L=1.2.

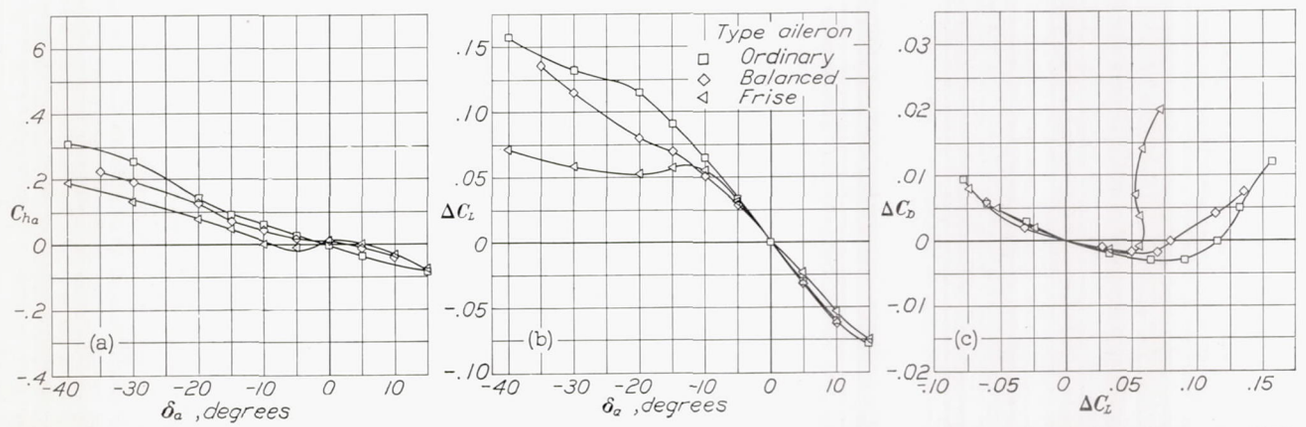

(a) Variation of aileron hinge-moment coefficient with aileron deflection.

(b) Variation of lift-coefficient increment with aileron deflection.

(c) Variation of drag-coefficient increment with lift-coefficient increment.

FIGURE 28.—Characteristics of various balanced ailerons on N. A. C. A. 23012 airfoil. C_L=0.2.

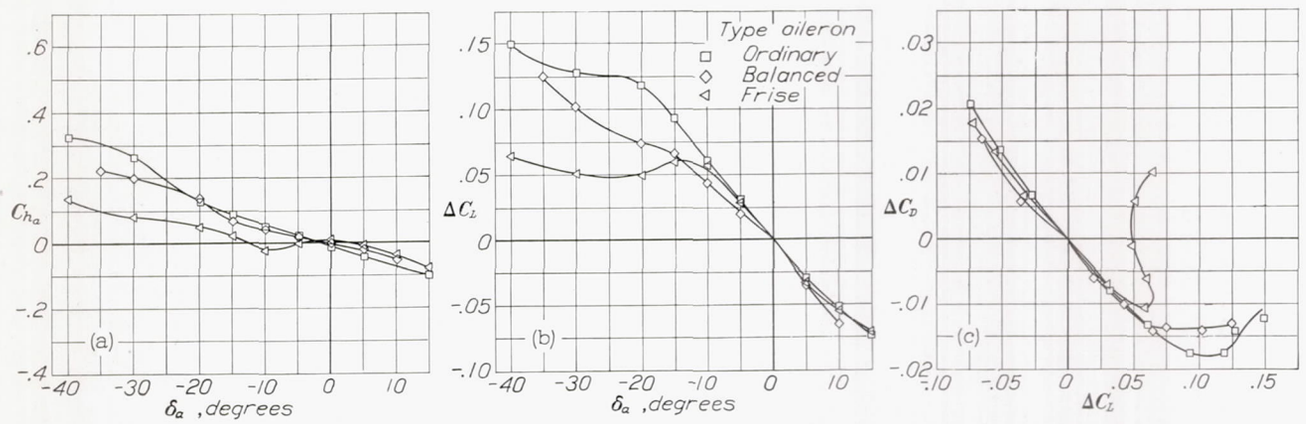

(a) Variation of aileron hinge-moment coefficient with aileron deflection.

(b) Variation of lift-coefficient increment with aileron deflection.

(c) Variation of drag-coefficient increment with lift-coefficient increment.

FIGURE 29.—Characteristics of various balanced ailerons on N. A. C. A. 23012 airfoil. C_L=0.7.

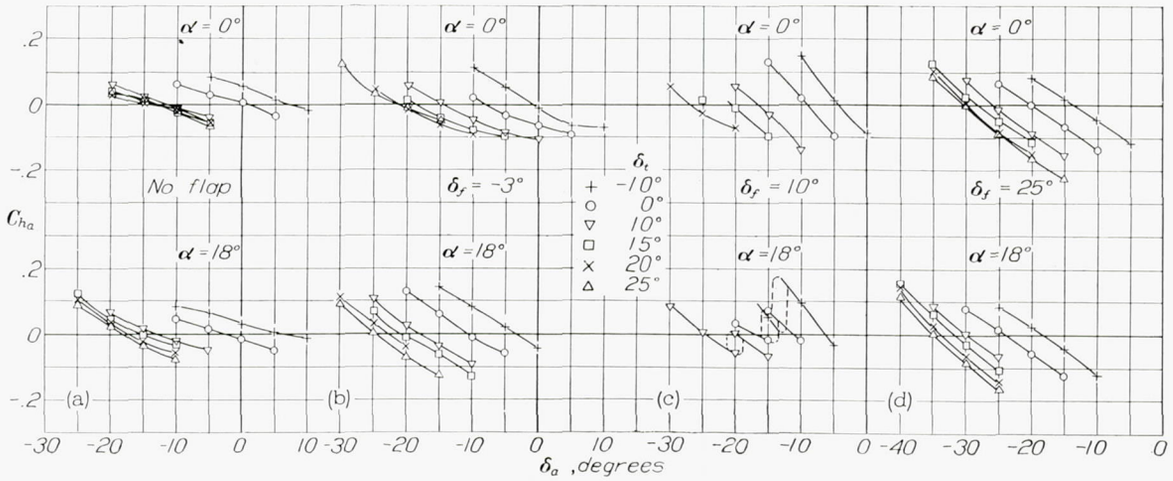

FIGURE 30.—Hinge-moment coefficients of a 0.12 c_w ordinary aileron with 0.15 c_a tab, mounted on an N. A. C. A. 23012 airfoil with and without a 0.20 c_w external-airfoil flap.

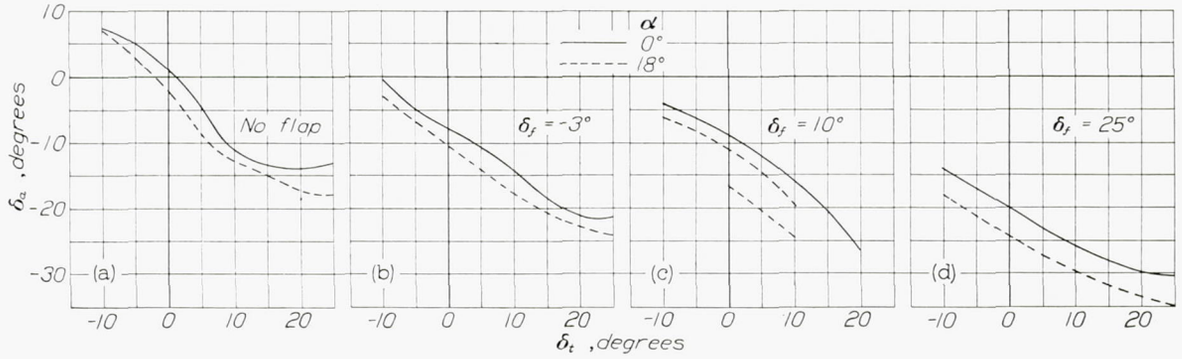

FIGURE 31.—Variation of aileron floating angle with tab deflection; 0.12 c_w ordinary aileron on an N. A. C. A. 23012 airfoil with and without a 0.20 c_w external-airfoil flap.

An unconventional method, subsequently explained, of using the tab to obtain aileron balance dictated the method adopted for presenting the data for the model with the tabbed aileron. In figure 30 the variation of aileron hinge-moment coefficient with aileron deflection is shown for a series of tab deflections at several conditions of angle of attack and flap angle. Figure 31 has been replotted from the data of figure 30 to show the variation of aileron floating angle with tab angle, the data for the model both with and without the flap being included. A drag test made at an air speed of 80 miles per hour with the aileron neutral, the flap both removed and set at the high-speed angle, and the model set at 0° angle of attack indicated that very small drag increments would result from a 20° deflection of the tab. The maximum increment of section profile-drag coefficient obtained was 0.0002, which lies within the limits of accuracy of the test.

DISCUSSION

As previously noted, the present investigation in one of its phases extended the investigation of the N. A. C. A. 23012 airfoil equipped with the N. A. C. A. 23012 external-airfoil flaps (reference 4) to include a flap having a 0.30 c_w chord. The methods used in selecting a desirable location of the flap-hinge axis and in obtaining and presenting the results directly paralleled those described in reference 4. Further, the data considered most significant for the airfoil with the 0.20 c_w flap have been transferred directly into this report for purposes of unity and completeness.

The discussion in reference 4 sets forth certain advantages of the external-airfoil type of wing-flap combination, principally in connection with its ability to produce high lift coefficients with relatively small increases of profile-drag coefficient. Figure 32 indicates the relative value of the 0.20 c_w and 0.30 c_w flaps in producing this effect. The curves are "envelope polars," obtained by fairing an envelope around the polar curves for various settings of the flap. The envelope polars thus show the minimum section profile-drag coefficient that can be obtained at any lift coefficient of which the wing-flap combination is capable. The graph demonstrates that the characteristics of the 0.30 c_w flap arrangement are at least as good as those of the 0.20 c_w flap arrangement and may be slightly better in certain particulars other than the maximum lift coefficient, in which the 0.30 c_w flap is definitely superior.

The better rounding of the polar for the 0.30 c_w flap, which gives it a slightly lower drag in the lift range normally used in take-off and simultaneously would permit a steeper gliding angle to be obtained at lift coefficients near the maximum, is believed to result from the different positioning of the hinge relative to the flap. The use of a hinge location for the 0.20 c_w flap similar to that for the 0.30 c_w might give a polar of more nearly similar shape. The effect on the maximum lift and minimum drag coefficients should not be adverse. No direct experimental evidence on this point was obtained, but comparison of the contour charts when they were used for selection of the hinge axis of the 0.30 c_w flap indicated the possibility.

It may be inferred from the observed variation of lift coefficient with flap angle and angle of attack that an airfoil and an external-airfoil flap act mutually to suppress the tendency of the flow to separate from their upper surfaces and thus delay stalling until a high lift coefficient is reached. An important phase of this action lies in the effect of the slot in producing a considerably higher speed of flow past the trailing edge of the airfoil than would exist with the flap absent. It therefore appears that ailerons placed on the trailing edge of an airfoil equipped with an external-airfoil flap are located in an especially effective position as compared with those located on a plain airfoil. On an ordinary airfoil it is known that the flow passes the trailing edge with little more than the free-stream velocity; in addition, the aileron may suffer from separation at angles somewhat below the stall. Under comparable conditions with the flap in action, it is apparent that the flow past the aileron has been accelerated and that the tendency to separation in this region has been suppressed. It therefore appears that such an aileron is in an excellent location for producing relatively large rolling-moment coefficients when the combination is developing a high lift coefficient. Reference to the flap-load data of reference 4 further shows that the flap carries very small forces when it is set for high speed: As a first approximation with the flap thus set the main airfoil may be considered an independent airfoil without appendages. It can then be inferred that deflection of the flap from the high-speed to the maximum-lift angle should cause a progressive increase in the effectiveness of the ailerons.

The foregoing considerations serve to clarify in part the variation of rolling-moment coefficient with flap deflection shown in figures 16 to 23. It is evident that as the flap is deflected the ailerons do gain considerably in effectiveness at a given lift coefficient of the wing-flap combination. The data reveal an additional simultaneous effect that serves further to improve the aileron effectiveness. As the aileron is deflected upward it bends the flow upward and reduces the lift. At the same time the size of the slot is considerably increased and the flow, tending to follow the lower surface of the aileron, encounters the flap at an increased angle of attack. At a certain point in the aileron travel the slot effectiveness has been reduced and the angle of attack of the flap sufficiently increased to cause the flap to stall, resulting in a further reduction in lift and increase in drag.

Inspection of figures 16 to 23 shows that this effect occurs at smaller aileron deflections as the flap approaches the maximum-lift angle, where the slot size is most critical. In figure 17, for example, the sharp rise in the rolling-moment curve, which is associated with the stalling of the flap, occurs at an aileron deflection of about 12° up when the flap is down 10°, at 5° up when the flap is down 20°, and so on. It is evident that this effect, which further increases the rolling moment and also reduces the adverse yawing moment, likewise comes into action progressively as the flap is deflected from the high-speed to the high-lift condition. When the flap has passed the maximum lift angle (see fig. 17, $\delta_f=55°$), the sudden increase of rolling moment

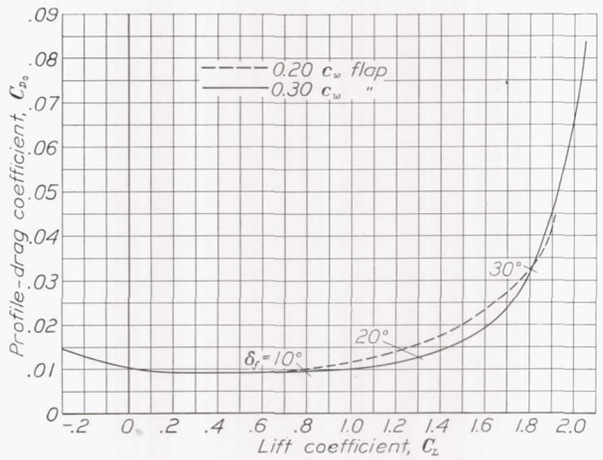

FIGURE 32.—Envelope polars for N. A. C. A. 23012 airfoil with 0.20 c_w and 0.30 c_w external-airfoil flaps. Effective Reynolds Number, approximately 1,000,000.

fails to appear because the flap is already stalled with the aileron neutral.

In connection with the effect of the stalling of the flap, it is noteworthy that the total lift of the flap is not lost, a low pressure is still maintained over the flap upper surface, and its effect in suppressing separation from the main airfoil is still active. Figure 14 shows the effect of deflecting the flap beyond its angle for maximum lift ($\delta_f=40°$ for the 0.30 c_w flap), in which case the flap stalled at a low angle of attack of the combination. Here the maximum lift coefficient was reduced approximately 0.3 by the stalling of the flap. As the maximum increase of $C_{L_{max}}$ produced by the flap in this case is 0.9, it is clear that about two-thirds of the flap effect remains after the flap has stalled. At still larger deflections the slot is completely ineffective, and it can be seen that the external-airfoil flap is then equivalent to a split or Zap flap with a small gap between it and the wing.

Thus far the discussion has tended to bring out considerations favorable to combinations of airfoils, external-airfoil flaps, and ailerons. Certain undesirable consequences of the foregoing considerations must also be recognized. It has been pointed out that ailerons of a given size on a wing with external-airfoil flaps can produce more rolling moment than normal ailerons of the same size on a plain wing. For application to airplane design it might be concluded that satisfactory control could be obtained with smaller ailerons by using them in combination with an external-airfoil flap. Such a conclusion is modified, however, by another important factor: The data (figs. 16 and 17) show that the effect of the flap is not active near the stalling lift coefficient with the flap at the high-speed angle; thus, ailerons of reduced area would be relatively weak in this condition.

The location of the aileron in relatively high-speed flow clearly must lead to increases of hinge moment as well as of rolling moment. Comparison of the lift increment per unit hinge moment of the present ailerons (fig. 24) with that for ordinary ailerons (fig. 28) indicates that with the flap in the high-speed setting the present ailerons are inferior. Since a large part of airplane operation would involve use of the ailerons with the flap at the high-speed setting, it seems desirable that the hinge moments of these ailerons be reduced to values comparable with those of ordinary ailerons for a given rolling moment. These considerations, which were first apparent when the tests of the standard model were compared with generally known characteristics of ordinary ailerons, led directly to the tests of the various balanced ailerons on the wide-chord model.

A study of some unpublished pressure-distribution data for airfoils with external-airfoil flaps suggested that a balance extending ahead of the aileron nose might serve to reduce the aileron hinge moments. Such a balance normally adds an appreciable amount of drag, but the provision of "curtains" covering most of the gap should eliminate the drag increment and still permit the pressures to act on the balance area. The arrangement finally selected, designated the "balanced aileron" in figure 3, was provided with such a balance and could be deflected between a 40° up and 15° down angle without encountering the curtains. Ordinary and Frise ailerons were included to provide a direct comparison with the tests on the standard model and with the action of a balance now in general use.

A slight reduction of hinge moment per unit deflection was obtained from the balanced aileron, but the lift increment per unit deflection likewise decreased from that obtained with the ordinary aileron, resulting in no actual improvement. The loss of lift increment suggests that there was more leakage between the balance nose and the airfoil than existed in the case of the plain aileron. This loss might be regained by the use of some system for sealing the clearance and some advantages thereby obtained. The present results, however, suggest that this form of balance does not merit general application at the present time though further development might render it very useful for wings either with or without external-airfoil flaps.

The data obtained for the Frise aileron clearly illustrate its action. As the aileron is deflected upward the nose drops into the flow below the wing, and the aileron "digs in," giving a mild degree of overbalance. As the nose becomes well extended, the upper surface of the aileron is vented to the lower; the resulting flow between the lower and upper surfaces markedly reduced the effectiveness of the ailerons. Simultaneously, the drag is increased by the disturbance to the flow, which would produce a favorable yawing moment such as has generally been observed in the use of Frise ailerons. In spite of the favorable effect on yawing moment, the Frise ailerons do not appear to be of appreciable interest in the present connection on account of their effect in reducing the maximum available rolling moment and in having a tendency to overbalance in the initial stages of deflection.

Another method of reducing stick forces involves the use of a differential linkage for aileron operation. (See references 2 and 8.) The differential linkage interacts with any tendency of the ailerons to float up from neutral to produce a reduction in the stability of the complete aileron system. In the tests reported in reference 2 certain cases were found where the stability became negative, i. e., the system was actually overbalanced. In this case the action is readily visualized: The downgoing aileron reaches its maximum travel, with the drive crank at dead center, before the upgoing aileron has reached its natural upfloating angle. Thus, the upgoing aileron is trying to deflect itself still farther when the downgoing aileron can no longer exert a restoring moment; the aerodynamic forces thus tend to move the stick away from its neutral position. When the upfloating angle of the ailerons is known, a differential can be selected that will interact with the upfloating tendency to produce a lesser reduction of stability than that previously described. The stick forces are thus reduced without producing overbalance by a proper coordination of the differential linkage with the aileron floating angle and the slope of the curve of hinge moment with deflection.

Jones and Nerken (reference 8) have investigated the properties of differential linkages and give formulas and charts for the proper coordination of the important factors. They have further suggested, in the case of ailerons having a large variation of floating angle with angle of attack, the use of a tab mounted on each aileron to bias the aileron floating angle to a desirable value. In the case of the present type of aileron, this suggestion appears to be especially useful, since other considerations militate against complete freedom of

the designer in selecting a differential linkage suited purely to the aileron characteristics. As the floating angle of these ailerons varies with angle of attack and flap angle, it would be desirable to have the differential vary accordingly. This arrangement would not be feasible, and the tab is therefore used to provide the desired floating angle and thus avoid the necessity for a varying differential. The desirability of preventing the trailing edge of the downgoing aileron from passing the leading edge of the flap indicates a linkage that would reach dead center at a small downward aileron deflection. Tbis result, in turn, indicates that the upgoing aileron deflection will not be large when the downgoing aileron reaches dead center and that large upfloating angles (over 20°, for example) will tend to produce overbalance.

It is evident from the data for the standard model (figs. 16 to 24) and from the foregoing discussion that the ailerons operated by a differential linkage (which apparently is vital to their successful application) would be abnormally heavy in high-speed flight and might become overbalanced in low-speed flight with the flap down. The data of figure 31 show, however, that throughout the normal-flight range the size of tab tested is capable of bringing the aileron upfloating angle within the desired range (15° to 20°).

It should be noted that in this application both tabs are deflected the same amount in the same direction and the tab deflection (with respect to the aileron chord line) remains constant for a given setting of the flap regardless of aileron deflection. It is apparent that this is a highly unconventional application of a tab—the tab merely serves to bias the aileron floating angle and is not used to produce a moment about the aileron hinge opposing the aileron hinge moment, which is the normal use of tabs. The method presented in reference 8, together with the data of figure 31, provides a means of designing a lateral-control system having low stick forces and using the ailerons with the external-airfoil flap in the high-speed and high-lift settings.

In the intermediate range of flap settings (for which hinge moments were measured only on the tabbed aileron) an additional difficulty in connection with the use of the present ailerons became apparent. The data for the tabbed aileron with the flap deflected 10° (fig. 30 (c)) show that "hysteresis" appears in the variation of aileron hinge moment with deflection. This effect is attributed to the phenomenon of flap stalling: As the aileron moves away from the flap, the flow leaves the flap upper surface, relieving the aileron hinge moment and then, as the aileron returns, the flow is restored at a different deflection, producing the observed hysteresis. The appearance of the phenomenon with the tab neutral indicates that it would appear equally on an untabbed aileron although no tests were made of the untabbed ailerons with the flap in the intermediate angle range. The data in figure 30 (c) for the tab 0°, flap 10° down, indicate the range in which the hysteresis appears to be near 15° up aileron deflection, corresponding approximately to the aileron deflection at which the sharp rise of rolling moment took place (see fig. 18 (a), $\delta_f = 10°$) in the tests of the standard model. It is anticipated that this discontinuous action, which might affect the rolling moment as well as the stick force, would be very disconcerting to a pilot. Although no further investigation was undertaken at the time, it is possible that scale effects and the use of a gradually stalling airfoil section for the flap might tend to smooth out the discontinuity.

Certain immediate possibilities of overcoming the difficulty may deserve mention. Use of the flap in only the high-speed and maximum-lift settings with a rapid change between them should permit the pilot to avoid the range in which the hysteresis appears. On very large airplanes in which the ailerons might be power-driven and no aileron "feel" would reach the pilot's control, the aileron deflection would be susceptible of accurate control without reference to the stick forces. In this case, the hysteresis should not be an appreciable disadvantage. This consideration also suggests the use of an irreversible operating mechanism for smaller airplanes, in which case the hysteresis might be noticeable but should not tend to produce disconcerting movements of the airplane. Such an arrangement should also tend to suppress aileron flutter, some tendency to which was noticed in the tests when the aileron trailing edge closely approached the flap leading edge.

CONCLUDING REMARKS

The data obtained in the present investigation indicate the following generalizations. An N. A. C. A. 23012 airfoil equipped with a 0.30 c_w N. A. C. A. 23012 external-airfoil flap, like the similar combination with a 0.20 c_w flap, gave characteristics favorable to speed range, to low power requirements in flight at high lift coefficients, and to low flap-operating moments. The aerodynamic qualities of the combination make it especially suitable for the application of ailerons mounted on the trailing edge of the main airfoil, providing a means of lateral control consistent with the use of full-span external-airfoil flaps. This possibility gives the external-airfoil flap an advantage in speed-range capabilities over such flaps as the ordinary and simple split types, which, when used with ordinary ailerons, sacrifice part of their span for the provision of lateral control.

The results from the narrow-chord long-span ailerons here investigated indicated large rolling-moment coefficients at lift coefficients corresponding to flight conditions ranging from high speed to minimum speed. The adverse yawing moments tended to be somewhat less than those of ordinary ailerons giving the same rolling moment. In general, they agree with Munk's formula for induced yawing moment at low values of the rolling moment; as the rolling moment is increased, they tend to become more favorable.

Three definite difficulties to be anticipated in the application of the combination of ailerons with external-airfoil flaps are indicated. First, the ailerons are relatively weak in producing rolling moment when the wing is near the stalling angle of attack with the flap in the high-speed setting. Second, the variation of aileron hinge moment with angle of attack and flap setting is such as to cause relatively large stick forces in the high-speed range and to cause overbalance near the stall with the flap in the high-lift setting. Third, a discontinuity of hinge moment, and possibly of rolling moment, occurs as the ailerons are deflected with the flap in the intermediate-angle range. The investigation indicated that nose balances and Frise balances were ineffective in reducing the stick forces required for a given control effectiveness in the high-speed condition. The use of a tab to bias the aileron floating angle together with a differential aileron motion provides a means of obtaining reduced stick forces in the high-speed condition and of avoiding overbalance in the high-lift condition. Further research and application to experimental designs should serve to determine the importance of the anticipated difficulties in actual use and should establish more clearly the merit of the combination of ailerons and external-airfoil flaps for airplane-design application.

LANGLEY MEMORIAL AERONAUTICAL LABORATORY,
NATIONAL ADVISORY COMMITTEE FOR AERONAUTICS,
LANGLEY FIELD, VA., *March 12, 1937.*

APPENDIX

EFFECT OF JET BOUNDARIES AND ASPECT RATIO ON MEASURED ROLLING- AND YAWING-MOMENT COEFFICIENTS

As previously noted in the text, the use of standard airfoils for tests of airfoils with external-airfoil flaps in the 7- by 10-foot tunnel led to the use of geometric aspect ratios of 5.0 and 4.61 for the combinations tested in the present investigation. Although main airfoils of larger aspect ratio could have been constructed, considerations of model deflection, comparison of plain-airfoil test data, and economy dictated the method adopted. It was recognized, however, that the variation of lift-curve slope and of induced drag with aspect ratio would result in measured rolling- and yawing-moment coefficients not directly comparable with data from tests of airfoils of aspect ratio 6. Corrections based on present knowledge of induced-flow phenomena were therefore devised to permit such comparisons.

CORRECTION OF ROLLING-MOMENT COEFFICIENT

Pearson (reference 9) has carried out a general solution of the lift distribution for wings with ailerons, from which he obtained an equation for the rolling moment

$$L=2qb^2(k\delta)F_2$$

where q is the dynamic pressure.

b, the wing span.

δ, the aileron deflection.

and F_2, a factor (presented in chart form) depending on plan form, aspect ratio, and ratio of total aileron span to total wing span.

The factor k is a section characteristic for an airfoil with a flap or aileron and is equal to the change of angle of attack equivalent to a given aileron deflection divided by the given aileron deflection. This value may also be expressed as the ratio of the section lift-curve slopes $\frac{dc_l}{d\delta}\Big/\frac{dc_l}{d\alpha_0}$. (The lower-case letters represent airfoil section characteristics; thus c_l is the section lift coefficient, C_L the wing lift coefficient, and C_l the wing rolling-moment coefficient.) The equation thus represents the total rolling moment as the rolling moment to be expected from the change of airfoil section when the aileron is deflected, reduced by a factor to allow for the induced rolling moment resulting from wing plan-form effect.

Computing the rolling-moment coefficient from Pearson's formula, the equation

$$C_l=2A(k\delta)F_2$$

is obtained, where A is the aspect ratio. By the use of this relation and the designation of the values appropriate to two different aspect ratios as subscript A_1 and subscript A_2, it is possible to obtain a factor for the rolling-moment coefficient measured for a wing of $A=A_1$ to express the rolling-moment coefficient for a wing of $A=A_2$ under otherwise identical conditions, as follows:

$$C_{l_{A_2}}=C_{l_{A_1}}\times\frac{A_2F_{2_{A_2}}}{A_1F_{2_{A_1}}}\times\frac{(k\delta)_{A_2}}{(k\delta)_{A_1}}$$

But it has been pointed out that k depends only on the airfoil section characteristics and therefore does not change with A. Thus, at a given value of aileron deflection

$$(k\delta)_{A_1}=(k\delta)_{A_2}$$

and

$$C_{l_{A_2}}=C_{l_{A_1}}\times\frac{A_2F_{2_{A_2}}}{A_1F_{2_{A_1}}}$$

Factors for the particular values of A in question were calculated from the formula using values of F_2 obtained from the reference and cross-plotted against A. The final correction formulas used were as follows: for the airfoil with the 0.20 c_w flap and 0.12 c_w ailerons

$$C_{l_{A=6}}=1.08\ C_{l_m}$$

and for the airfoil with the 0.30 c_w flap and 0.13 c_w ailerons

$$C_{l_{A=6}}=1.12\ C_{l_m}$$

The subscript m signifies the value measured in the wind tunnel.

The error produced by the jet boundaries in the measured rolling-moment coefficient has been estimated from the formula of reference 10; it amounts to less than 1 percent of the measured coefficient and is conservative for prediction of flight rolling moments. This correction is consequently considered negligible.

CORRECTION OF YAWING-MOMENT COEFFICIENT

Munk (reference 11) expressed the induced yawing-moment coefficient of a wing with ailerons having equal up-and-down deflections as

$$C_{n_i}=-\frac{3C_l'}{\pi A}\times C_L$$

(It should be noted that there is a disagreement of sign with the original published formula; the sign has been changed to agree with the standard N. A. C. A. sign convention for moments.) This formula may be used to compute the change of C_{n_i} resulting from a given change of aspect ratio; this computation is directly

analogous to the well-known one for the change of induced drag coefficient with aspect ratio.

The jet-boundary effect on the induced yawing-moment coefficient results from the change in local wind direction (α_{i_t}, the standard angle-of-attack correction) with respect to the model resulting from the limited extent of the air stream. Through this effect the rolling-moment vector is rotated through the angle α_{i_t}, resulting in a component in the yawing-moment direction

$$C_{n_{i_t}}=\alpha_{i_t}\times C_l$$

The jet-boundary correction factor for the 7- by 10-foot tunnel is equal to 0.165 in the formula $\alpha_{i_t}=\delta_\alpha\frac{S}{C}C_L$. (See reference 2.)

The total induced yawing-moment coefficient of a model in the 7- by 10-foot tunnel may then be expressed as

$$C_{n_i}=-\left[\frac{3C_{l_m}}{\pi A_m}\times C_L\right]-\left[0.165\frac{S}{C}\times C_{l_m}\times C_L\right]$$

or

$$C_{n_i}=-C_{l_m}\times C_L\left(\frac{3}{\pi A_m}+0.165\frac{S}{C}\right)$$

The profile yawing-moment coefficient is then

$$C_{n_0}=C_{n_m}+C_{l_m}\times C_L\left(\frac{3}{\pi A_m}+0.165\frac{S}{C}\right)$$

For $A=6$

$$C_{n_i}=-C_{l_{A=6}}\times C_L\times\frac{3}{6\pi}$$

but

$$C_{l_{A=6}}=\beta C_{l_m}$$

where

$$\beta=\frac{A_2F_{2_{A_2}}}{A_1F_{2_{A_1}}}$$

the rolling-moment coefficient correction factor previously developed. Thus for $A=6$

$$C_{n_{i_{A=6}}}=-C_{l_m}\times C_L\times\frac{3\beta}{6\pi}$$

and since

$$C_{n_{A=6}}=C_{n_0}+C_{n_{iA=6}}$$

$$C_{n_{A=6}}=C_{n_m}+C_{l_m}\times C_L\left(0.165\frac{S}{C}+\frac{3}{\pi A_m}-\frac{3\beta}{6\pi}\right)$$

Inserting appropriate values the following correction formulas were derived. For the airfoil with the 0.20 c_w flap and 0.12 c_w ailerons

$$C_{n_{A=6}}=C_{n_m}+0.0309\times C_{l_m}\times C_L$$

For the airfoil with the 0.30 c_w flap and 0.13 c_w ailerons

$$C_{n_{A=6}}=C_{n_m}+0.0418\times C_{l_m}\times C_L$$

In conclusion it should be noted that the foregoing corrections, which have been applied to all the rolling- and yawing-moment coefficients presented in this report, include the standard assumptions of induced flow and jet-boundary correction theory. They should therefore be regarded as first approximations rather than as rigorous expressions of the corrections that should be applied.

REFERENCES

1. Soulé, H. A., and McAvoy, W. H.: Flight Investigation of Lateral Control Devices for Use with Full-Span Flaps. T. R. No. 517, N. A. C. A., 1935.
2. Platt, Robert C.: Aerodynamic Characteristics of Wings with Cambered External-Airfoil Flaps, Including Lateral Control with a Full-Span Flap. T. R. No. 541, N. A. C. A., 1935.
3. Shortal, Joseph A.: Wind-Tunnel and Flight Tests of Slot-Lip Ailerons. T. R. No. 602, N. A. C. A., 1937.
4. Platt, Robert C., and Abbott, Ira H.: Aerodynamic Characteristics of N. A. C. A. 23012 and 23021 Airfoils with 20-Percent-Chord External-Airfoil Flaps of N. A. C. A. 23012 Section. T. R. No. 573, N. A. C. A., 1936.
5. Harris, Thomas A.: The 7 by 10 Foot Wind Tunnel of the National Advisory Committee for Aeronautics. T. R. No. 412, N. A. C. A., 1931.
6. Platt, Robert C.: Turbulence Factors of N. A. C. A. Wind Tunnels as Determined by Sphere Tests. T. R. No. 558, N. A. C. A., 1936.
7. Jacobs, Eastman N., and Sherman, Albert.: Airfoil Section Characteristics as Affected by Variations of the Reynolds Number. T. R. No. 586, N. A. C. A., 1937.
8. Jones, Robert T., and Nerken, Albert I.: The Reduction of Aileron Operating Force by Differential Linkage. T. N. No. 586, N. A. C. A., 1936.
9. Pearson, H. A.: Theoretical Span Loading and Moments of Tapered Wings Produced by Aileron Deflection. T. N. No. 589, N. A. C. A., 1937.
10. Biot, M.: Korrecktur für das Quermoment von Tragflügeln bei Untersuchungen im Windkanal mit Kreisquerschnitt. Z. F. M., 24. Jahrgang, Nr. 15, 14. August 1933, S. 410–411.
11. Munk, Max M.: A New Relation between the Induced Yawing Moment and the Rolling Moment of an Airfoil in Straight Motion. T. R. No. 197, N. A. C. A., 1924.

U. S. GOVERNMENT PRINTING OFFICE: 1937

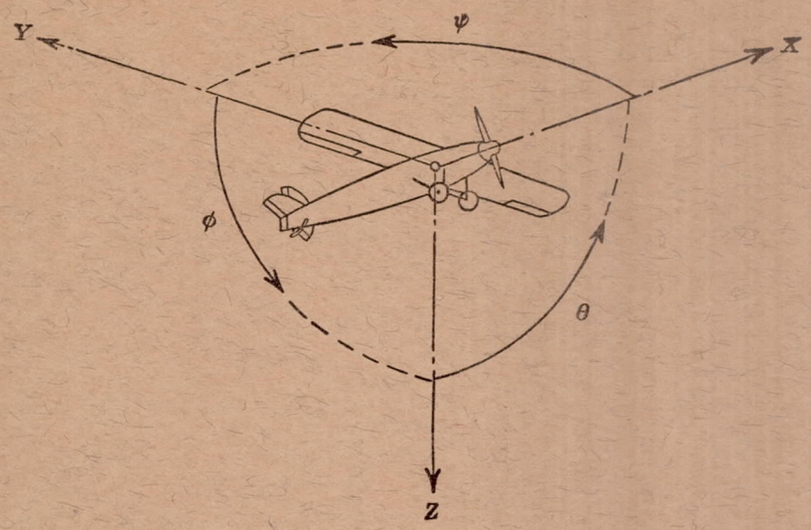

Positive directions of axes and angles (forces and moments) are shown by arrows

Axis		Force (parallel to axis) symbol	Moment about axis			Angle		Velocities	
Designation	Symbol		Designation	Symbol	Positive direction	Designation	Symbol	Linear (component along axis)	Angular
Longitudinal	X	X	Rolling	L	$Y \longrightarrow Z$	Roll	ϕ	u	p
Lateral	Y	Y	Pitching	M	$Z \longrightarrow X$	Pitch	θ	v	q
Normal	Z	Z	Yawing	N	$X \longrightarrow Y$	Yaw	ψ	w	r

Absolute coefficients of moment

$C_l = \frac{L}{qbS}$ (rolling) $\quad C_m = \frac{M}{qcS}$ (pitching) $\quad C_n = \frac{N}{qbS}$ (yawing)

Angle of set of control surface (relative to neutral position), δ. (Indicate surface by proper subscript.)

4. PROPELLER SYMBOLS

D, Diameter

p, Geometric pitch

p/D, Pitch ratio

V', Inflow velocity

V_s, Slipstream velocity

T, Thrust, absolute coefficient $C_T = \frac{T}{\rho n^2 D^4}$

Q, Torque, absolute coefficient $C_Q = \frac{Q}{\rho n^2 D^5}$

P, Power, absolute coefficient $C_P = \frac{P}{\rho n^3 D^5}$

C_s, Speed-power coefficient $= \sqrt[5]{\frac{\rho V^5}{P n^2}}$

η, Efficiency

n, Revolutions per second, r.p.s.

Φ, Effective helix angle $= \tan^{-1}\left(\frac{V}{2\pi r n}\right)$

5. NUMERICAL RELATIONS

1 hp.=76.04 kg-m/s=550 ft-lb./sec.

1 metric horsepower=1.0132 hp.

1 m.p.h.=0.4470 m.p.s.

1 m.p.s.=2.2369 m.p.h.

1 lb.=0.4536 kg.

1 kg=2.2046 lb.

1 mi.=1,609.35 m=5,280 ft.

1 m=3.2808 ft.